Structure Formation and Cosmology with high-z Clusters

Lecture Plan

Piero Rosati (ESO)

L1 : Introduction, observational techniques
- Observational definition, observable physical properties
- Methods for cluster searches - Cluster surveys
- Multi-wavelength observations of distant clusters

L2: Clusters as Cosmological Tools
- Constraining cosmological parameters with clusters
- The new population of high-z clusters

L3: Probing Dark Matter in Clusters
- Basics of gravitational lensing (strong and weak)
- Constraining DM density profiles in cores - ΛCDM predictions
- Clusters as gravitational telescopes

L4: Galaxy populations and evolution in distant clusters
- Star formation history of cluster galaxies
- Evolution as a function of environments
- Proto-clusters

XVI IAG/USP Advanced School on Astrophysics, Itatiba,
Brazil - Nov 5-9 2012

Mass-Energy density budget in the Universe governs the expansion history

$$\left(\frac{\dot{a}}{a}\right)^2 = H^2(z) = H_0^2[\Omega_M(1+z)^3+\Omega_R(1+z)^4+\Omega_\Lambda(1+z)^{3(1+w)}+(1-\Omega_0)(1+z)^2]$$

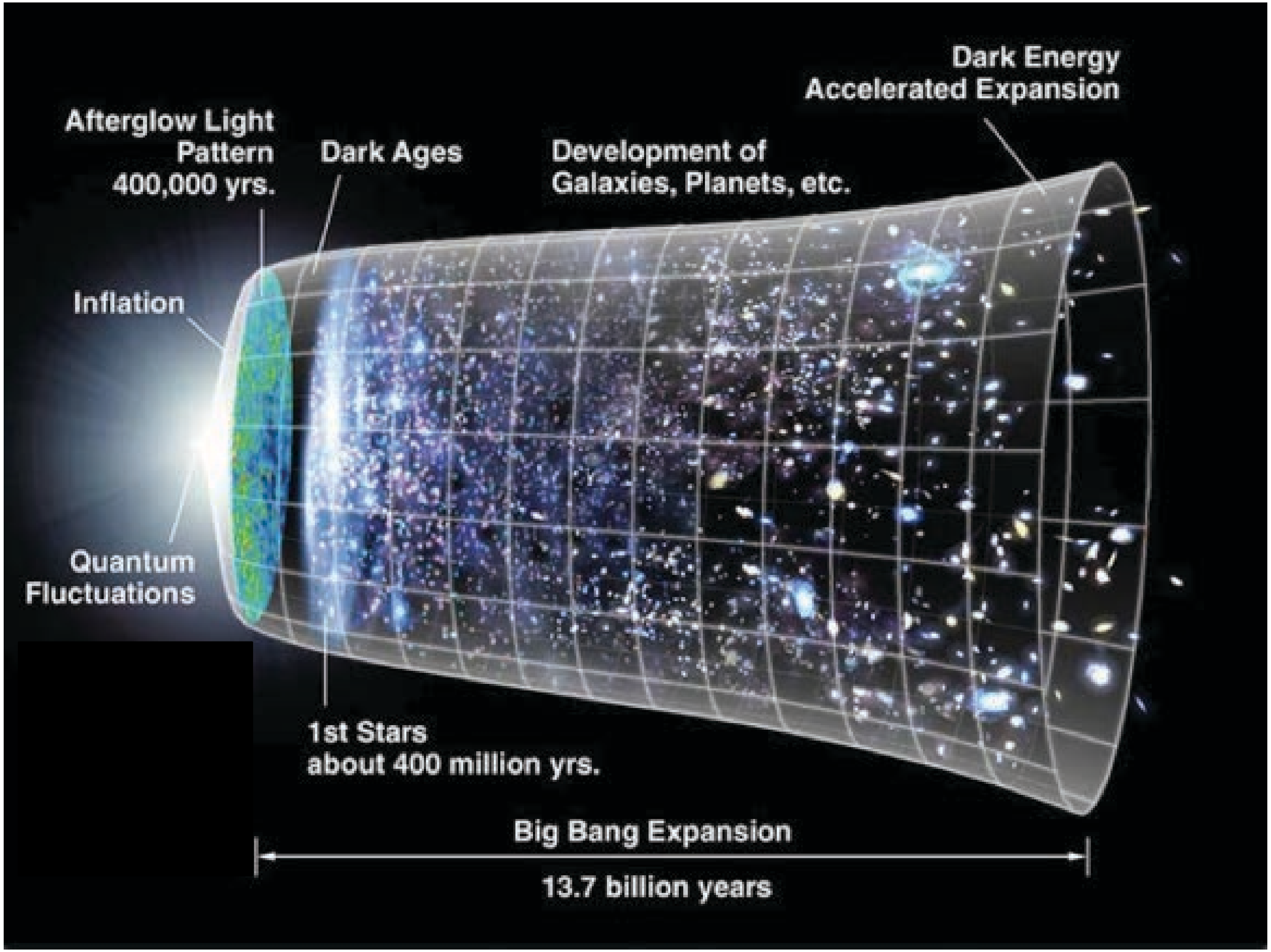

Mass-Energy density budget in the Universe governs the expansion history

$$\left(\frac{\dot{a}}{a}\right)^2 = H^2(z) = H_0^2[\Omega_M(1+z)^3+\Omega_R(1+z)^4+\Omega_\Lambda(1+z)^{3(1+w)}+(1-\Omega_0)(1+z)^2]$$

$$a \propto (1+z)^{-1} \qquad \Omega_0 = \Omega_M + \Omega_R + \Omega_\Lambda$$

$$\Omega_x = \rho_x/\rho_{cr}, \quad \rho_{cr} = 3H_0^2/8\pi G$$

$$\Omega_M = \Omega_b + \Omega_{CDM} \qquad \Omega_R = \Omega_{CMB} + \Omega_\nu$$

Dark Energy Eq. of state : $p = w\rho c^2, \qquad \rho \propto a^{-3(1+w)}$

Current concordance model

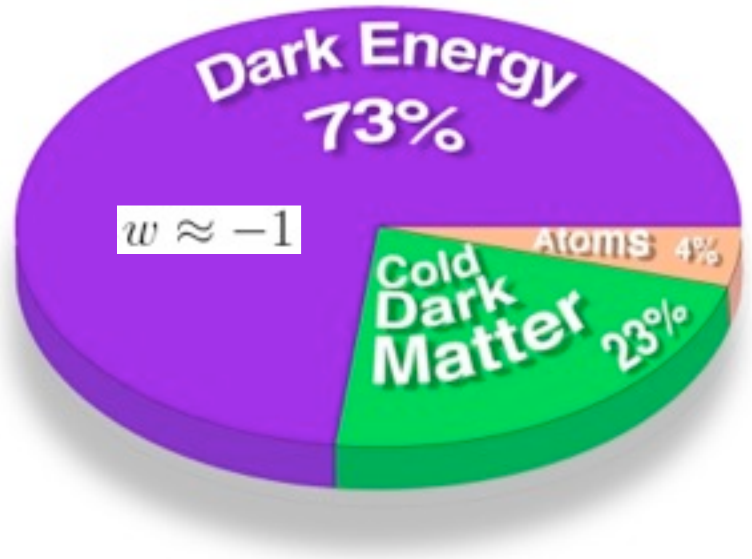

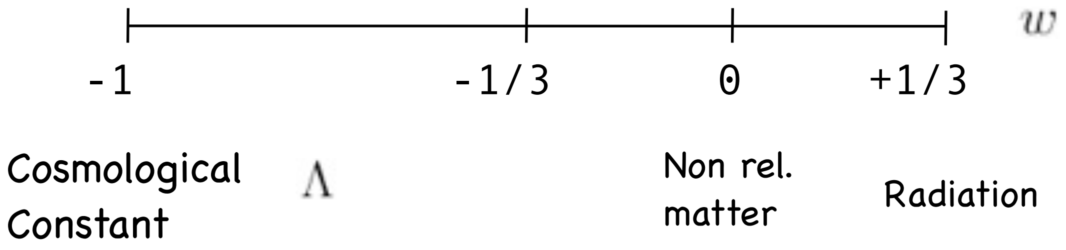

Cosmological Constant Λ

Non rel. matter

Radiation

Accelerating Universe if $w < -1/3$

$$\frac{\ddot{a}}{a} = -\frac{4}{3}\pi G\left(\rho + \frac{3p}{c^2}\right)$$

Each component in the energy density influences the expansion history of the Universe

Clusters are powerful probes of structure formation and cosmological models

1) Sensitive probe of the **dark sector** of the Universe (DM+DE)

Structure of DM halos (≲1 Mpc scale)

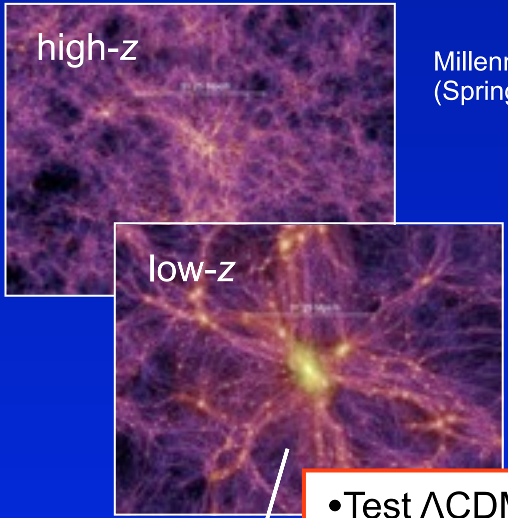

Millennium simulations
(Springel et al. 2005)

- Test ΛCDM predictions on DM density profiles
- Collision-less nature of DM?

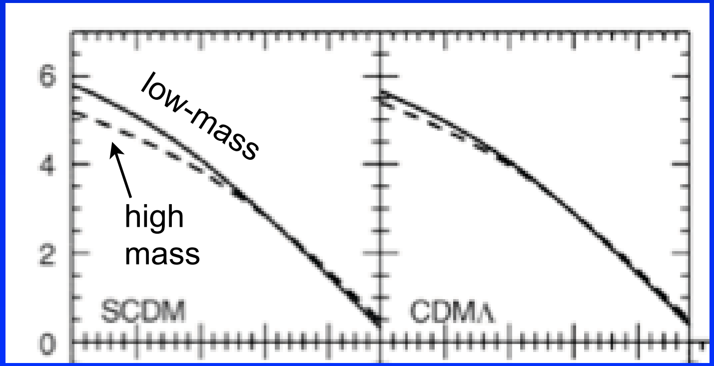

Mass function and distribution of DM halos (~ Gpc scale)

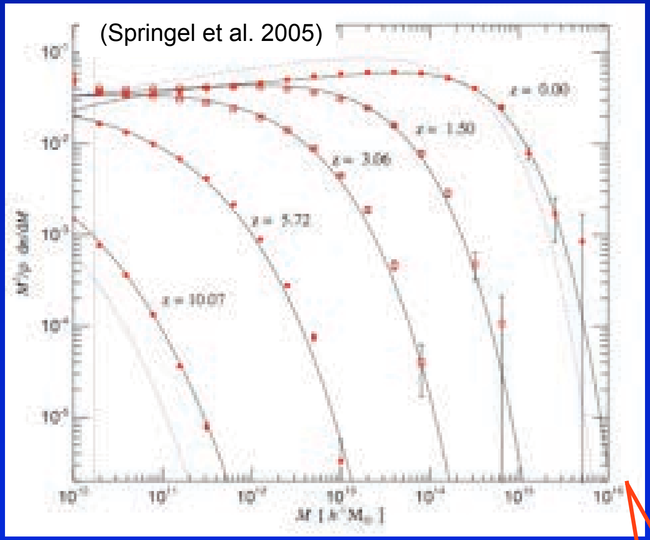
(Springel et al. 2005)

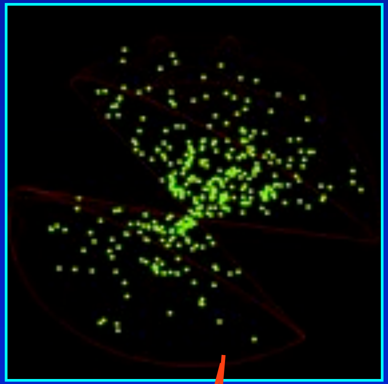

3D distribution

Keep indelible imprints of

1. background Cosmology
2. gravity law
3. initial conditions

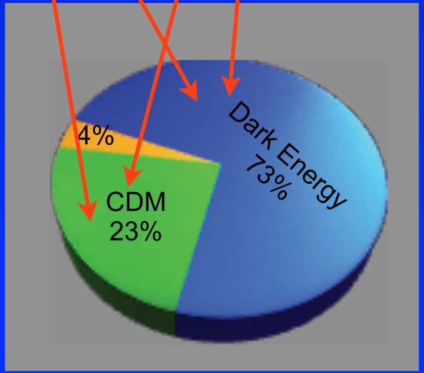

Test ΛCDM and GR:
<u>geometry</u> *vs* <u>growth</u>

Clusters are powerful probes of structure formation and cosmological models

1) Sensitive probe of the **dark sector** of the Universe (DM+DE)
2) Excellent places to trace the cosmic cycle of **baryons** and study the effect of galaxy formation and BH accretion on the ICM (feedback, Z enrichment)
   - Most of the baryons in clusters are detectable (X-ray gas + galaxies)
   - Almost closed box nature of deep potential wells make them ideal laboratories

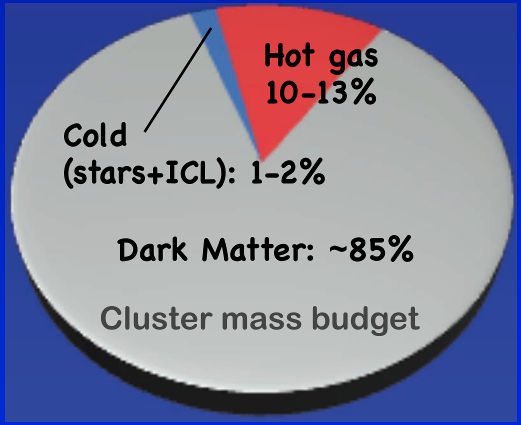

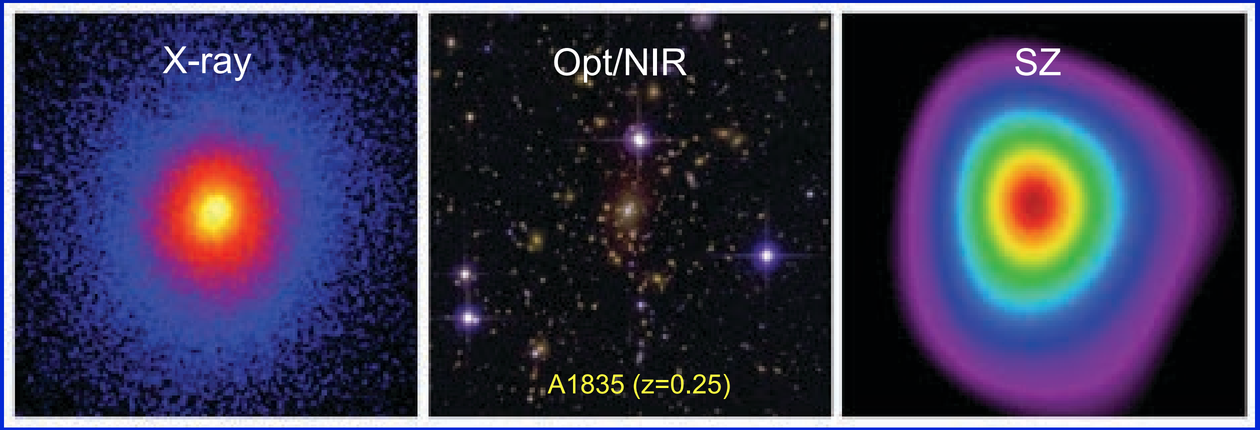

hot gas (X-ray, SZ)

galaxy over-densities (opt/IR)

Cluster searches

(DM) weak lensing

RGs/AGN as signposts for proto-clusters

The cosmic baryon budget

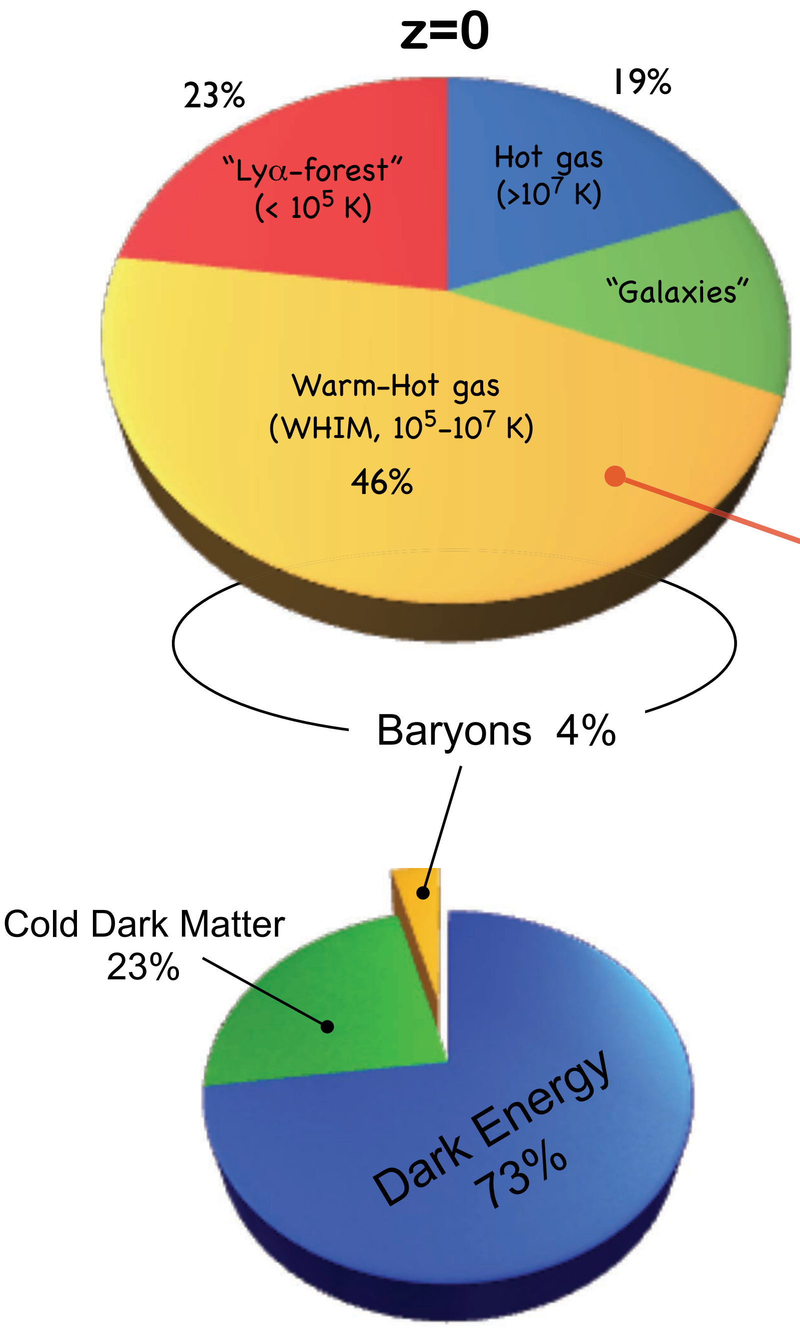

Mass-Energy density budget

$$\Omega_b = 0.045 \pm 0.002 \text{ (for h=0.72, from BBN \& WMAP)}$$

$$\Omega_{b,obs@\ z<1} \approx \Omega_* + \Omega_{HI} + \Omega_{H2} + \Omega_{Xray,cl} + \Omega_{Ly\alpha,f} \approx 0.02$$

Significant fraction of "missing baryons" at z~0 likely in filaments (WHIM)

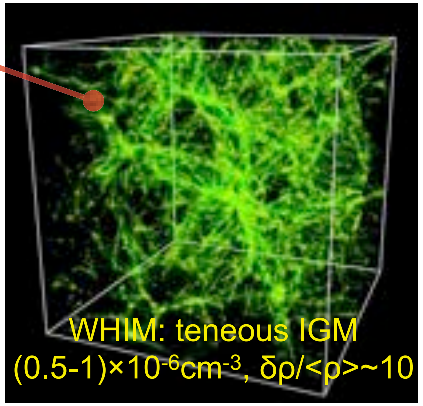

WHIM: teneous IGM
(0.5-1)×10^{-6}cm^{-3}, $\delta\rho/\langle\rho\rangle \sim 10$

The cosmic baryon budget

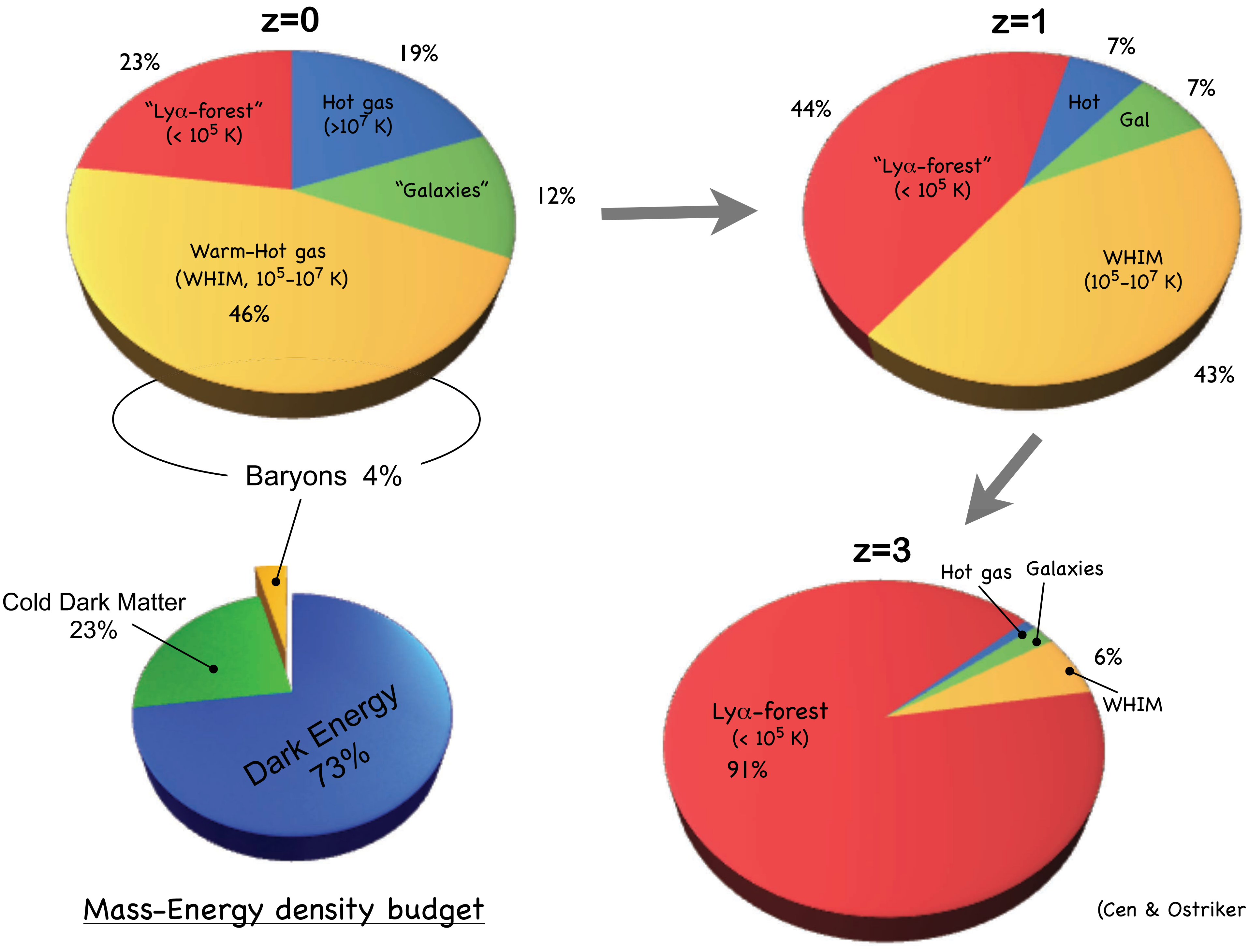

Mass-Energy density budget

(Cen & Ostriker 1999)

What about the distribution of baryons in clusters ?

Cluster baryon budget (Ettori 03, 08)

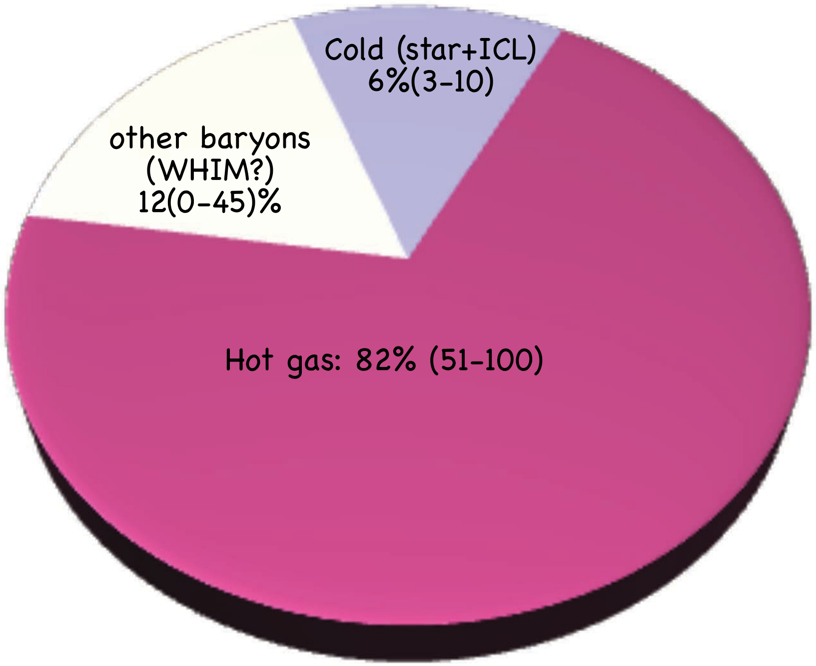

Cosmic baryon budget at z~0

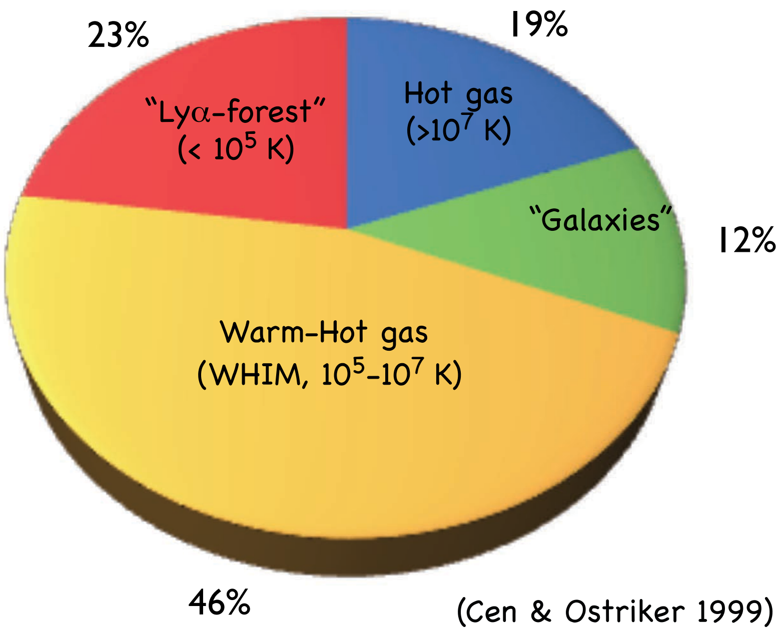

(Cen & Ostriker 1999)

- Most of the baryons in clusters can be observed:
  - X-ray gas + Massive (early-type) galaxies
  - However… only a few % of the galaxies are in clusters!

- The only places where one can have a full accounting of the intergalactic baryons, their thermal state, and their heavy-elements enrichments ➔ ideal place to study cooling and feedback processes (SN, AGN) which shape galaxy formation

Clusters of galaxies: the largest mass concentrations in the Universe

- **Concentration of** 100-1000 **galaxies**
- **Velocity dispersion (observed):** $\sigma_v \sim 1000$ km $s^{-1} \sim 1$ Mpc/Gyr
- **Size:** $R \sim 1$ Mpc $\Rightarrow$ the crossing time (lower limit to the relaxation time) is $t_{cross} = R/\sigma_v \sim 1$ Gyr $< t_H = 9.8\ h^{-1}$ Gyr $\Rightarrow$ **clusters dynamically relaxed**
- **Mass:** assuming virial equilibrium $\Rightarrow$ $M \simeq \frac{R\sigma_v^2}{G} \simeq \left(\frac{R}{1}\right)\left(\frac{\sigma_v}{10^3}\right)^2 10^{15}\,h^{-1}M_\odot$

  $\Rightarrow M = 10^{14}\text{-}10^{15}\ M_\odot$ $\Rightarrow \lambda_{init} \sim 10$ Mpc
- **Mass components:** $f_{baryons} \approx$ 10-15% ($f_{gas} \approx$10%, $f_{gal} \approx$ a few%), $f_{DM} \approx$ 80-90%
- **Intra-Cluster Gas: Temperature:** $T_X \approx$ 3-10 keV, $k_BT \simeq \mu m_p \sigma_v^2 \simeq 6\left(\frac{\sigma_v}{10^3}\right)^2$ keV

  SZ compt.param: $y \approx 10^{-4}$ $y_e = \int n_e \sigma_T dl \left(\frac{k_B T_e}{m_e c^2}\right) = \int d\tau_e \left(\frac{k_B T_e}{m_e c^2}\right)$

  Central density: $n_{gas,0} \approx 10^{-3}$ atoms/cm^3

  $\Rightarrow$ **fully ionized plasma, free-free bremsstrahlung + lines emission with:**

  $L_X \sim n_{gas}^2 \Lambda(T)\, V \sim 10^{43}\text{-}10^{45}$ erg s^{-1}

  Metallicity: ~0.3 solar (observed, from complex chemical evolution of galaxies)

Galaxy cluster “prototype”

Coma Galaxy Cluster

from POSS and ROSAT-All Sky

(Courtesy of H.Böhringer)

74 – 83% = Dark Matter
15 – 20% = hot gas
2 - 6% = galaxies

Gas T’s and system Masses depend on the depth of the potential well in a continuum from early-type galaxies to super clusters

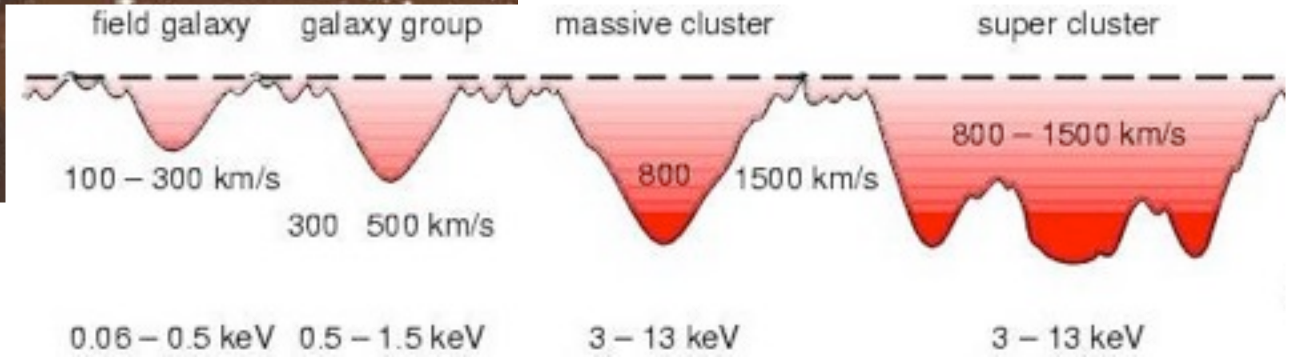

Observable Properties of Clusters

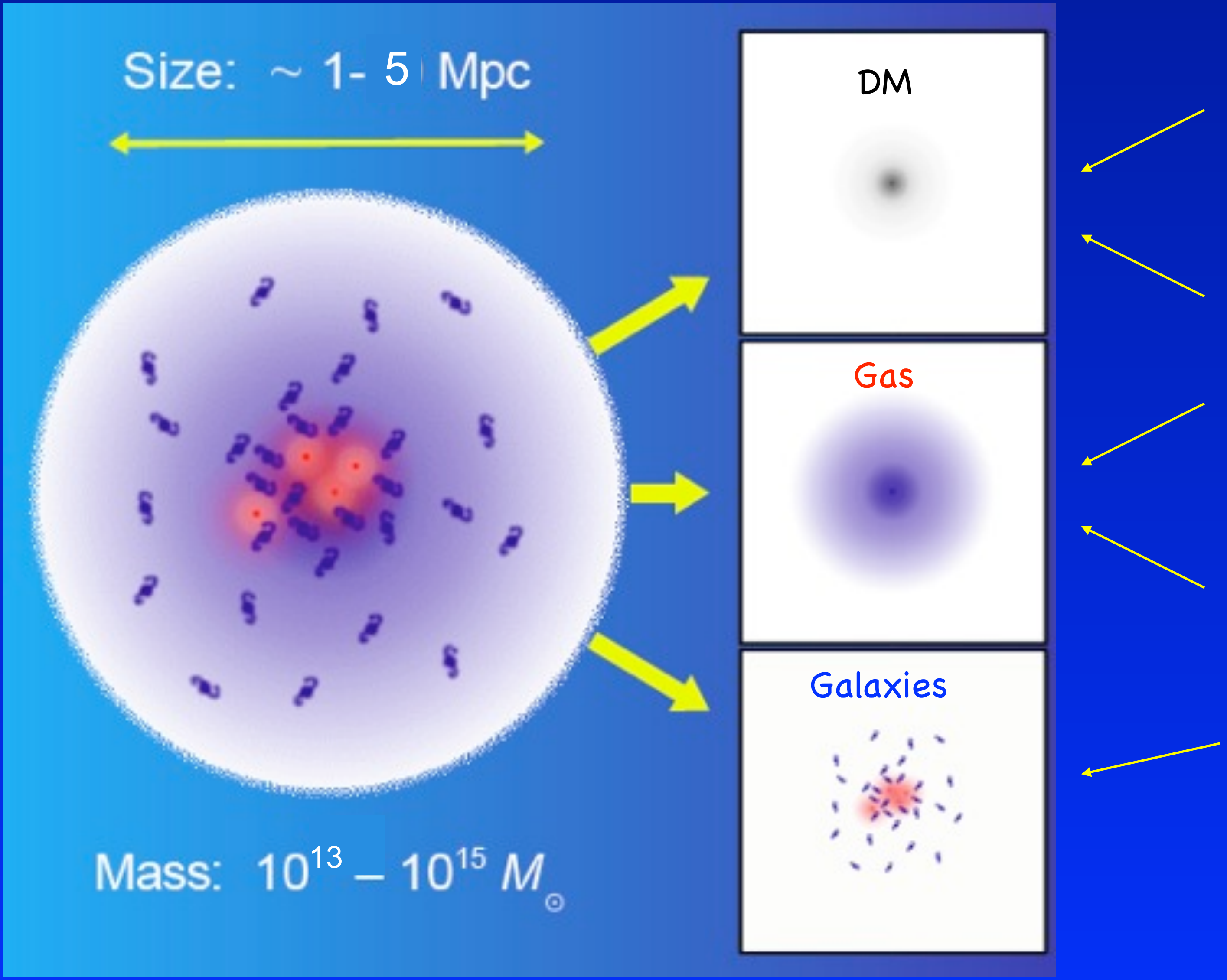

Lensing

Mass distrib./profiles
Nature of DM

Gal dynamics

X-ray

Thermodynamics/masses
metallicity

SZ effect

Multi-λ photometry
and spectroscopy

Stellar mass/ stellar pop.
Galaxy evolution, SF rates

Formation of Clusters

- Clusters form from collapse of cosmic matter over a region of several Mpc's
- Cosmic baryons follow the dynamically dominant dark matter during collapse
- Due to adiabatic compression and shocks generated by supersonic motions during shell crossing and virialization, a thin hot gas confined into their potential wells is formed and radiate in X-ray
  - some time before/during collapse the gas is enriched with metals by stellar processes (SN ejecta) and "pre-heated" by sources of non-gravitational energy
- ~10% of baryons remain locked in a cold phase into stellar systems (mostly old red massive galaxies after a few Gyrs)

Credit: Borgani et al. (2003): 10 Mpc comoving across, ~5 kpc resolution (SPH+cooling+SF+SN feedback)

Cluster searches

🟢 Pros 🔴 Cons

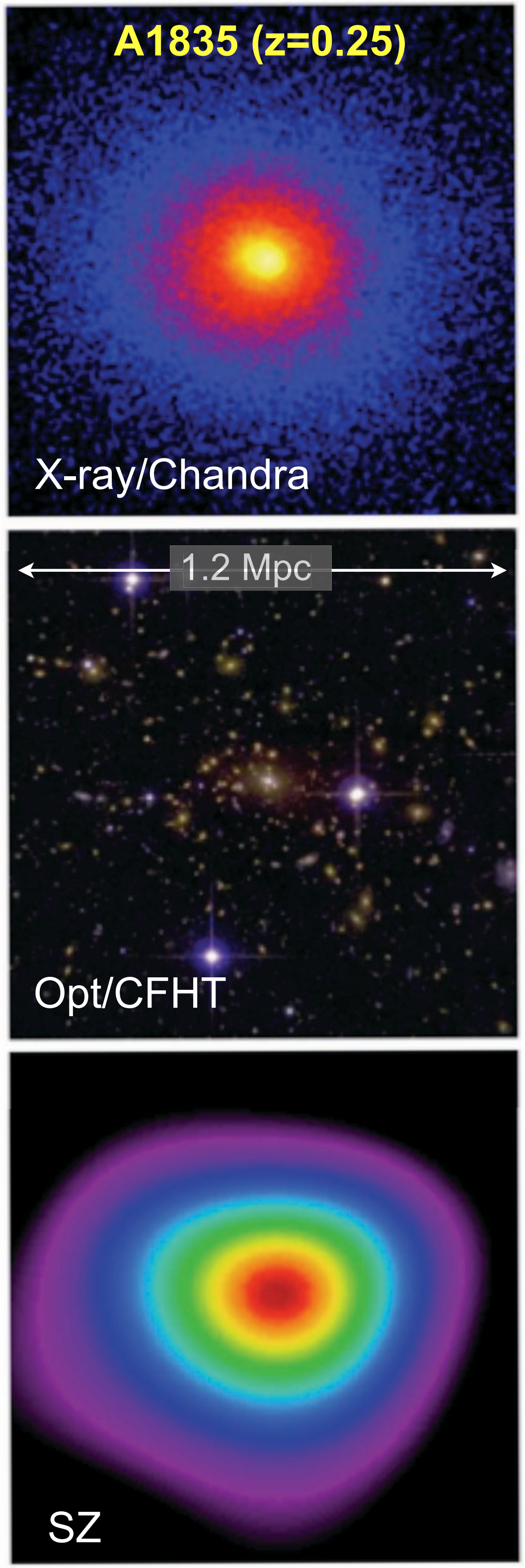

(Allen, Evrard, Mantz ARAA 2011)

X-ray

- 🟢 Clusters are high contrast extended objects in the X-ray sky ($L_x \sim \rho^2$)
- 🟢 L_x is a good Mass proxy, T and $Y_x = T \cdot M_{gas}$ better
- 🟢 Simple flux limited selection (survey volume) with *good angular resolution*
- 🔴 Difficult to cover very large areas with current missions
- 🔴 SB dimming limits effectivness at z>~1.5 with current X-ray missions

Galaxy overdensities

- 🟢 Contrast highly enhanced with extension to near-IR + color(s)
- 🟢 Easy to cover very large areas/volumes
  → massive rare systems
- 🔴 Projection effects, uncertain mass proxies
- 🔴 Search volume difficult to know with great accuracy
- 🔴 Difficult to identify virialized halos without massive spectroscopy

Cluster searches

🟢 Pros

🔴 Cons

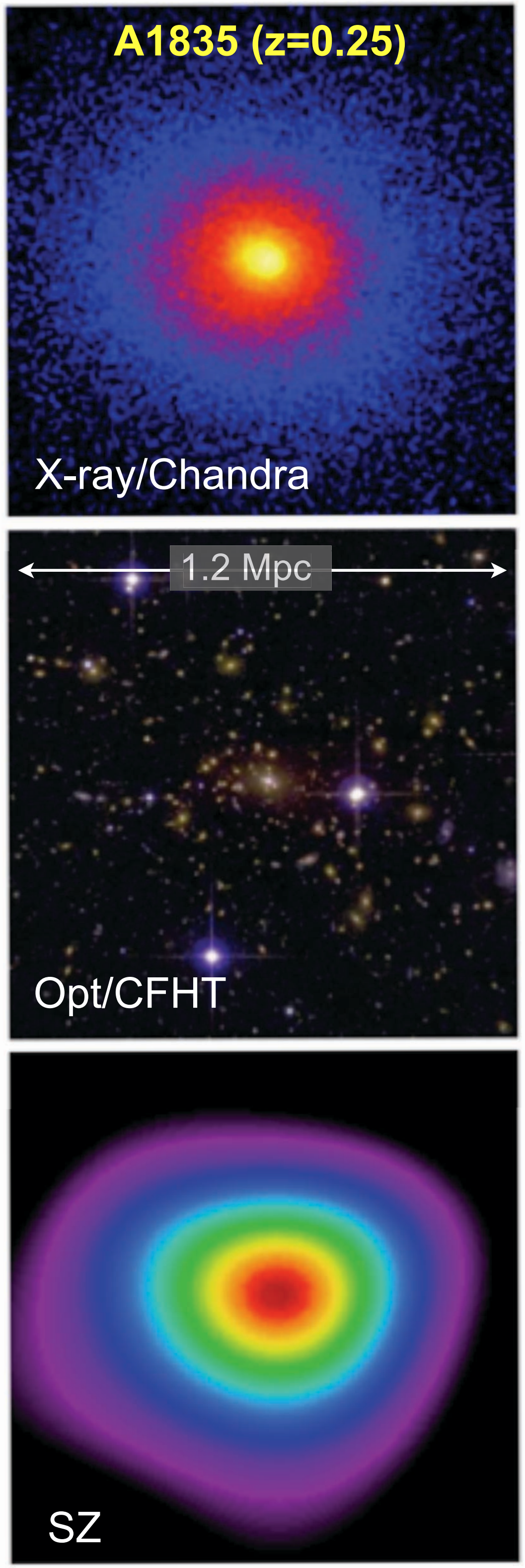

(Allen, Evrard, Mantz ARAA 2011)

X-ray

- 🟢 Clusters are high contrast extended objects in the X-ray sky ($L_x \sim \rho^2$)
- 🟢 L_x is a good Mass proxy, T and $Y_x = T \cdot M_{gas}$ better
- 🟢 Simple flux limited selection (survey volume) with *good angular resolution*
- 🔴 Difficult to cover very large areas with current missions
- 🔴 SB dimming limits effectivness at $z>\sim1.5$ with current X-ray missions

Galaxy overdensities

- MaxBCG sample from SDSS (Koester et al. 07, $\sim 10^4$ clusters) at $0.1<z<0.3$ with $N_{gal}>10$
- Red Cluster Sequence (RCS1,2; Gladders et al.): ~1000 sq.deg with CFHT/MegaCam in *griz*, ~500 clusters out to z~1
- IRAC Shallow/Deep Survey (Eisenhardt, Brodwin et al.), 30 cl at z>1

Cluster searches

🟢 Pros 🔴 Cons

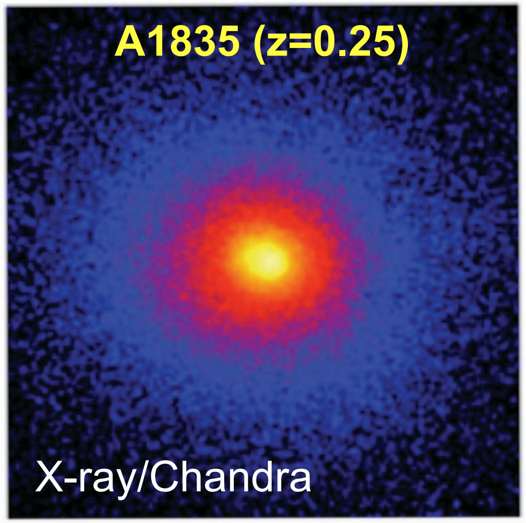

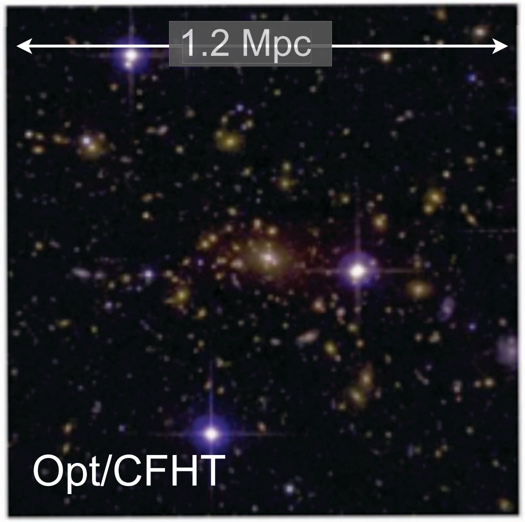

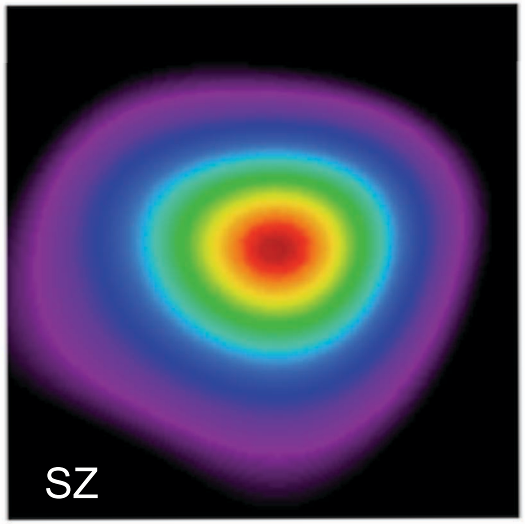

(Allen, Evrard, Mantz ARAA 2011)

X-ray

- 🟢 Clusters are high contrast extended objects in the X-ray sky ($L_x \sim \rho^2$)
- 🟢 L_x is a good Mass proxy, T and $Y_x = T \cdot M_{gas}$ better
- 🟢 Simple flux limited selection (survey volume) with *good angular resolution*
- 🔴 Difficult to cover very large areas with current missions
- 🔴 SB dimming limits effectivness at z>~1.5 with current X-ray missions

Galaxy overdensities

- MaxBCG sample from SDSS (Koester et al. 07, ~10^4 clusters) at $0.1<z<0.3$ with $N_{gal}>10$
- Red Cluster Sequence (RCS1,2; Gladders et al.): ~1000 sq.deg with CFHT/MegaCam in *griz*, ~500 clusters out to z~1
- IRAC Shallow/Deep Survey (Eisenhardt, Brodwin et al.), 30 cl at z>1

SZ effect

- 🟢 Sensitivity is almost independent of redshift
- 🟢 Integrated SZ signal Y= $\int \Delta_{SZ} d\Omega \propto \frac{N_{e,tot}\langle T_e\rangle}{D_A^2} \propto \frac{M\langle T_e\rangle}{D_A^2}$ → quasi-mass selected samples
- 🟢 Can cover large areas with $M_{\rm lim} \sim (2\text{-}3)10^{14}\ M_\odot$
- 🔴 Contamination from CMB anisotropies and radio/dusty sources (alleviated with multi-frequency observations and ~1' resolution)
- 🔴 Y-profile template-dependent selection function

Cluster searches

🟢 Pros

🔴 Cons

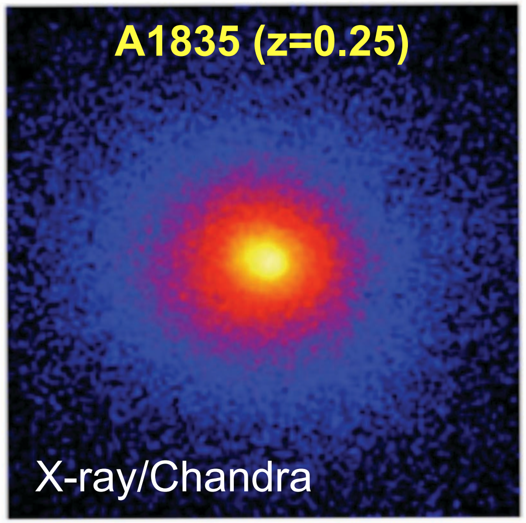

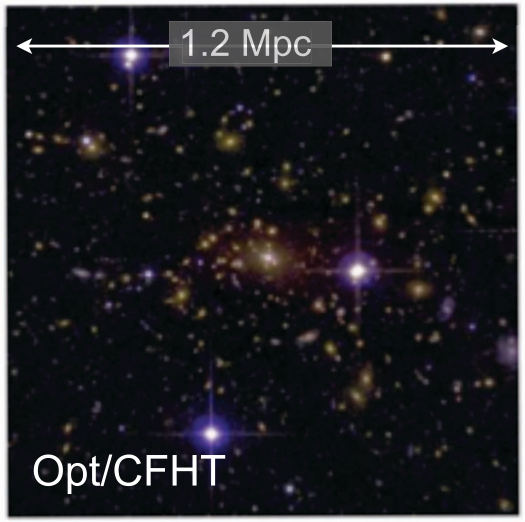

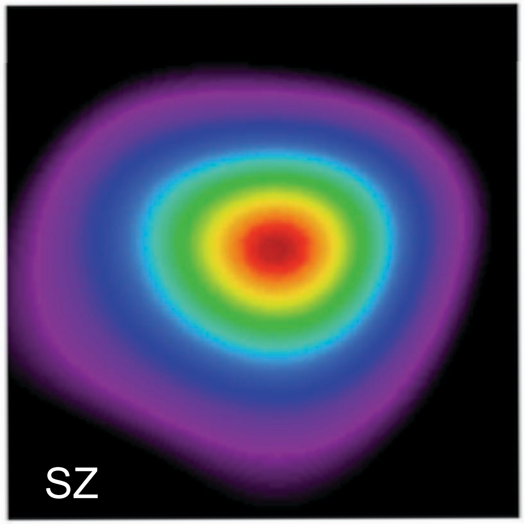

(Allen, Evrard, Mantz ARAA 2011)

X-ray

- 🟢 Clusters are high contrast extended objects in the X-ray sky ($L_x \sim \rho^2$)
- 🟢 L_x is a good Mass proxy, T and $Y_x = T \cdot M_{gas}$ better
- 🟢 Simple flux limited selection (survey volume) with *good angular resolution*
- 🔴 Difficult to cover very large areas with current missions
- 🔴 SB dimming limits effectivness at z>~1.5 with current X-ray missions

Galaxy overdensities

- MaxBCG sample from SDSS (Koester et al. 07, ~10^4 clusters) at 0.1<z<0.3 with $N_{gal}>10$
- Red Cluster Sequence (RCS1,2; Gladders et al.): ~1000 sq.deg with CFHT/MegaCam in *griz*, ~500 clusters out to z~1
- IRAC Shallow/Deep Survey (Eisenhardt, Brodwin et al.), 30 cl at z>1

SZ effect

- Planck ESZ sample at low-z
- SPT: 2500 (78) sq.deg with $M_{lim} \sim 2 \times 10^{14}\ M_\odot$ (Williamson et al. 2011)
- ACT: 455 sq.deg (Marriage et al. 2010) M_{lim} ~2x higher

Cluster searches (continued)

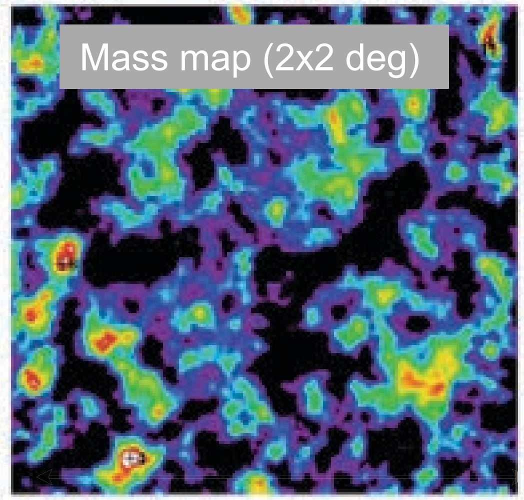

Weak Lensing (blind) searches

- ● Detection independent of dynamical state and baryon content in clusters (projected mass)
- ● Dark Lens Survey (KPNO, Tyson et al.) 20 deg^2, WL Blind Cl Survey with Subaru/SupCam (33 deg^2) best efforts so far
- ● Difficult from the ground (selection function depending on observing conditions), limited to z~0.8
- ● It will be powerful with a wide-field space surveys (e.g. Euclid)

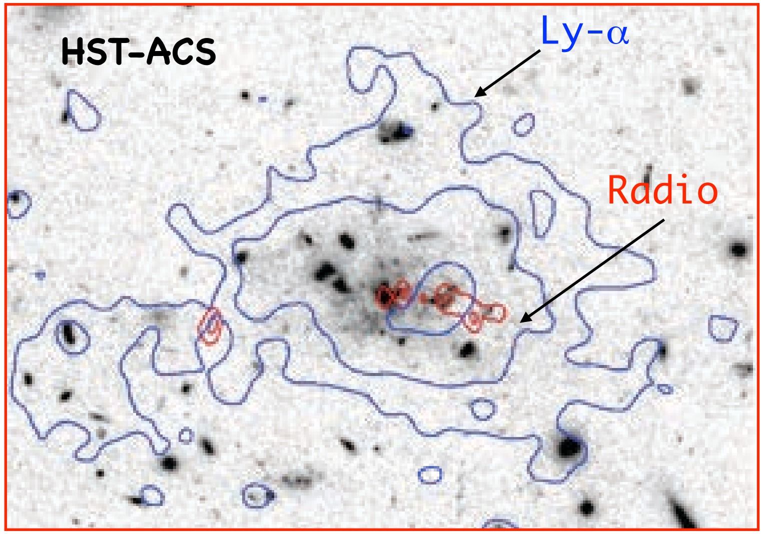

Overdensities around (high-z) radio sources

- Powerful FR-II radio galaxies (Miley et al.) at 2<z<4
- Low-power FR-I's as signposts (Chiaberge et al. 2010) 1.5<z<2

- ● Only method currently available to identify protoclusters at z~2-4 (plenty of spectroscopic support)
- ● No cosmology
- ● Challenging X-ray/SZ follow-up

Optical/near-IR selection

- Classic work of Abell, Zwicky on photographic plates
- Abell, Corwin, Olowin (1989): 4073 (+1174) clusters (foundation of modern studies)
- Similar work with automated algorithms on digitized photograpgic plates (e.g. Edinburgh-Durham Southern Galaxy Catalog) (Lumsden et al. 1992, Maddox et al. 1990)
- First cluster search at high-z (z=0.8) with deep photographic plates (Gunn et al. 1986, Couch et al. 1991)
- Similar work on CCD imaging material (e.g. Postman et al. 1996)
- Problems with estimate accurately the selection function (completeness?) esp. when only one band is used
- Projection effects increasingly severe at high redshifts, especially if only one band is used
- By moving to redder bands and imaging in different bands (up to near-IR bands) projection effects are mitigated and efficiency of cluster search is significantly boosted, particularly at high-z!
  - This has been exploited in recent years using wide-field multicolor imaging (e.g. RCS), including IR (2-5μ with Spitzer satellite)

Sloan Digital Sky Survey (SDSS) clusters

First release (2002):

- ✓ 1 Million galaxy spectra
- ✓ 10000 square degrees in the northern sky
- ✓ based on 5-color CCD photometry (2.5m telescope)

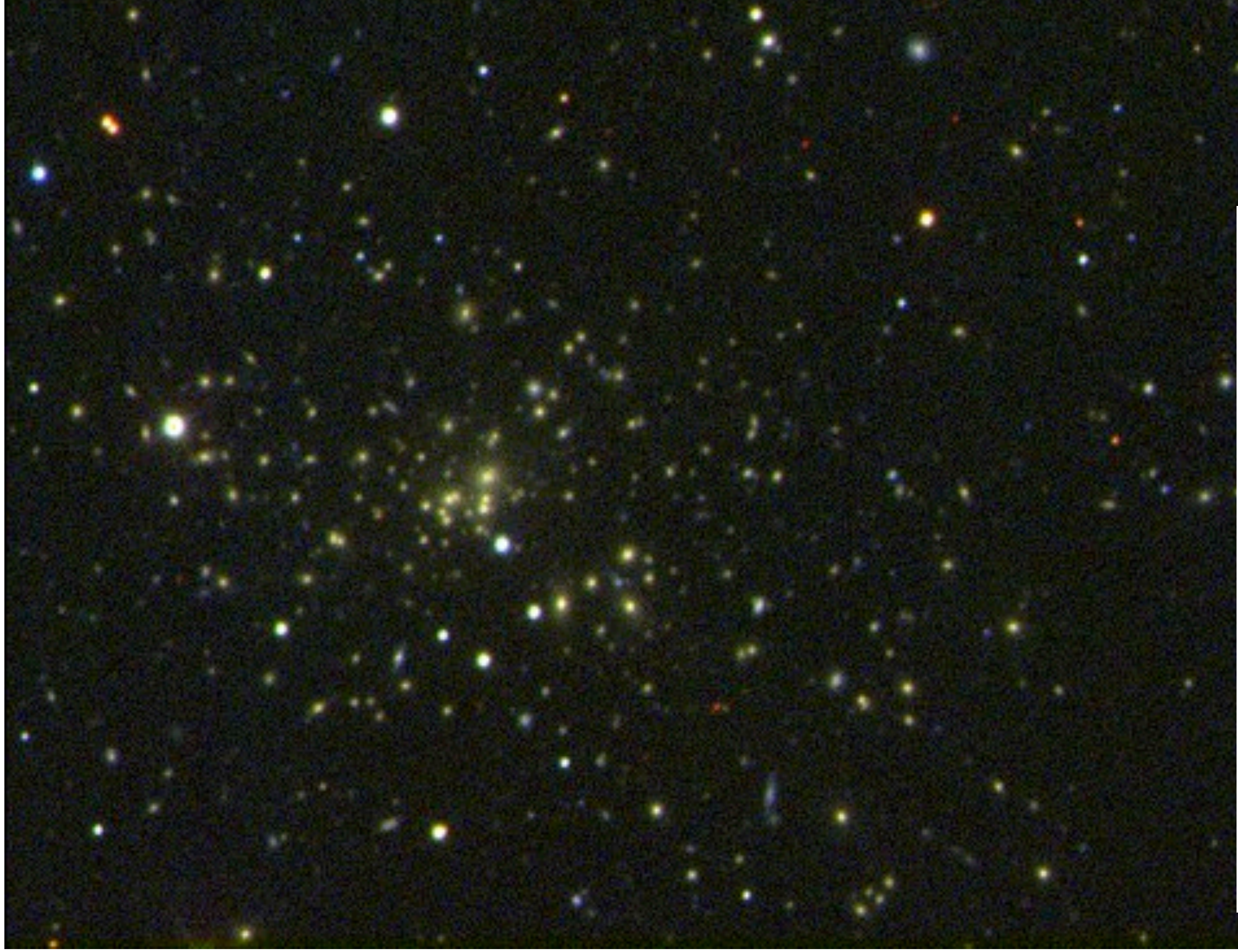

Goto et al. catalog (2003)
with cut&enhance technique
350 deg^2, ~360 candidates

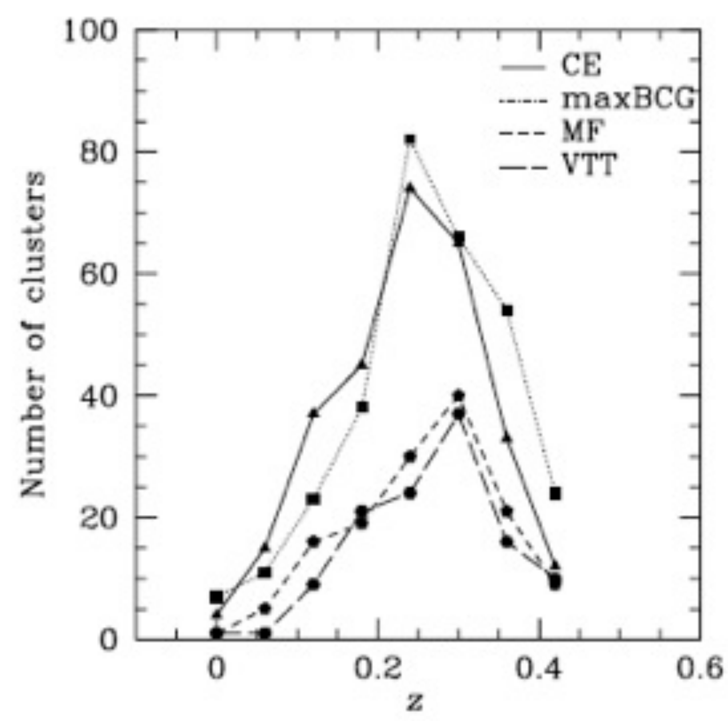

Distant clusters: blue/nearIR contrast

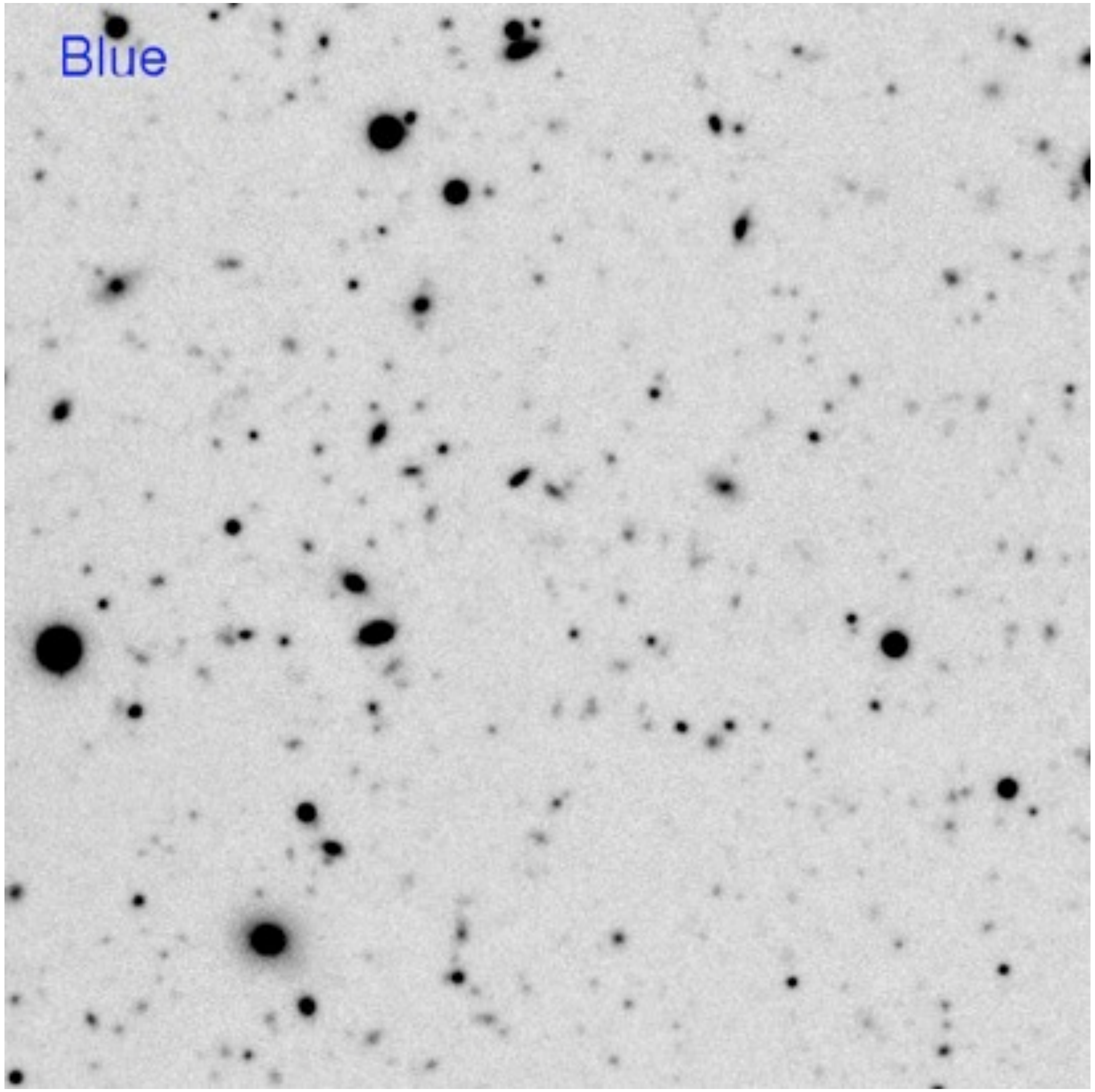

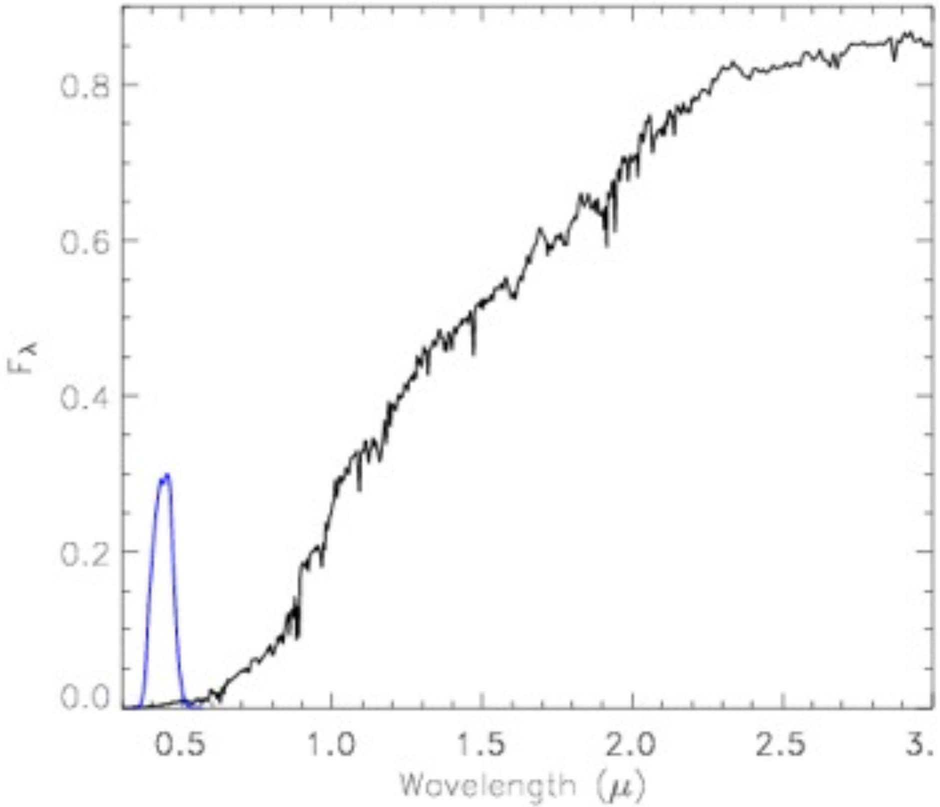

RDCS1252-29 @z=1.24 (Rosati et al.04)

Distant clusters: blue/nearIR contrast

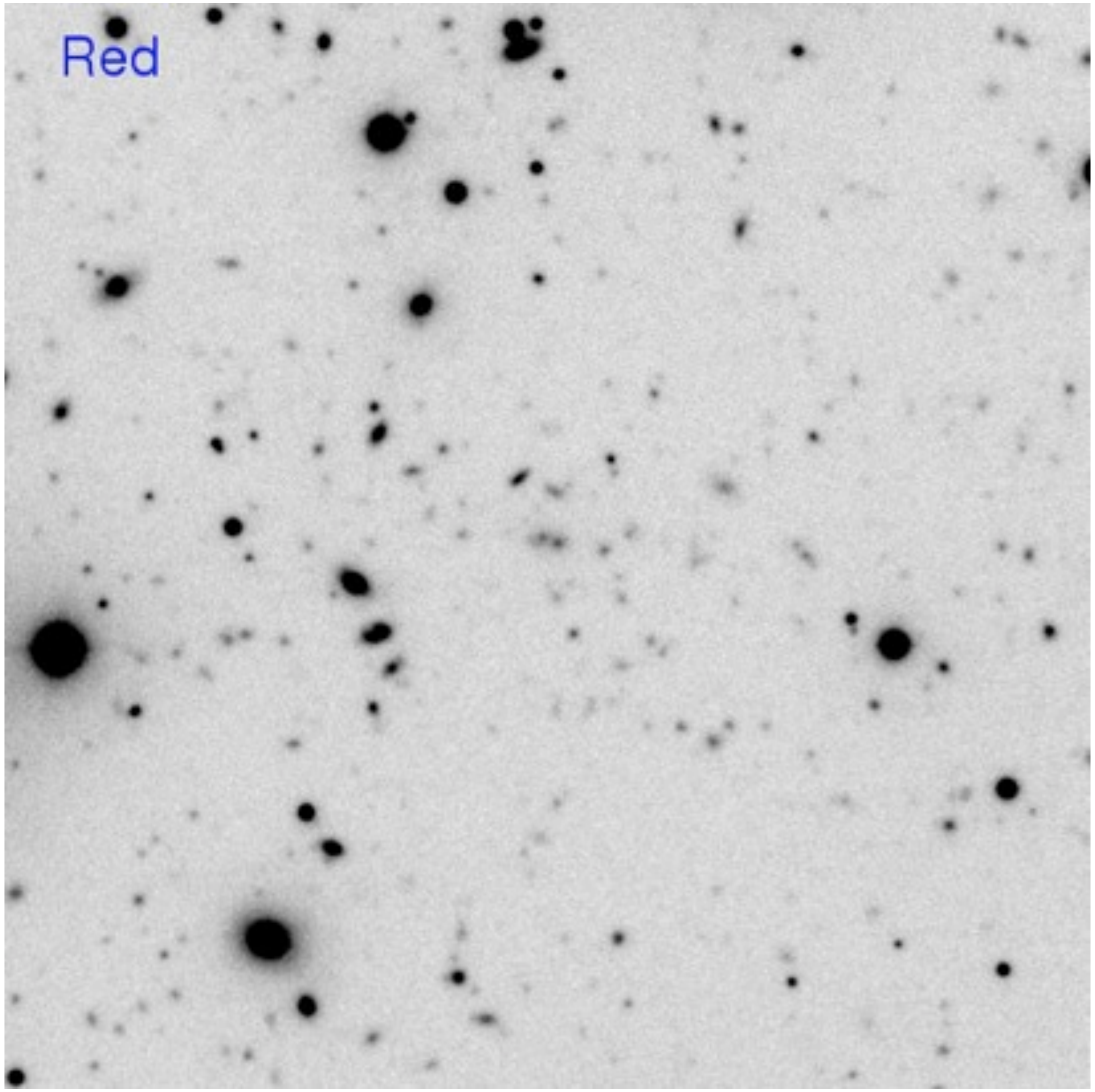

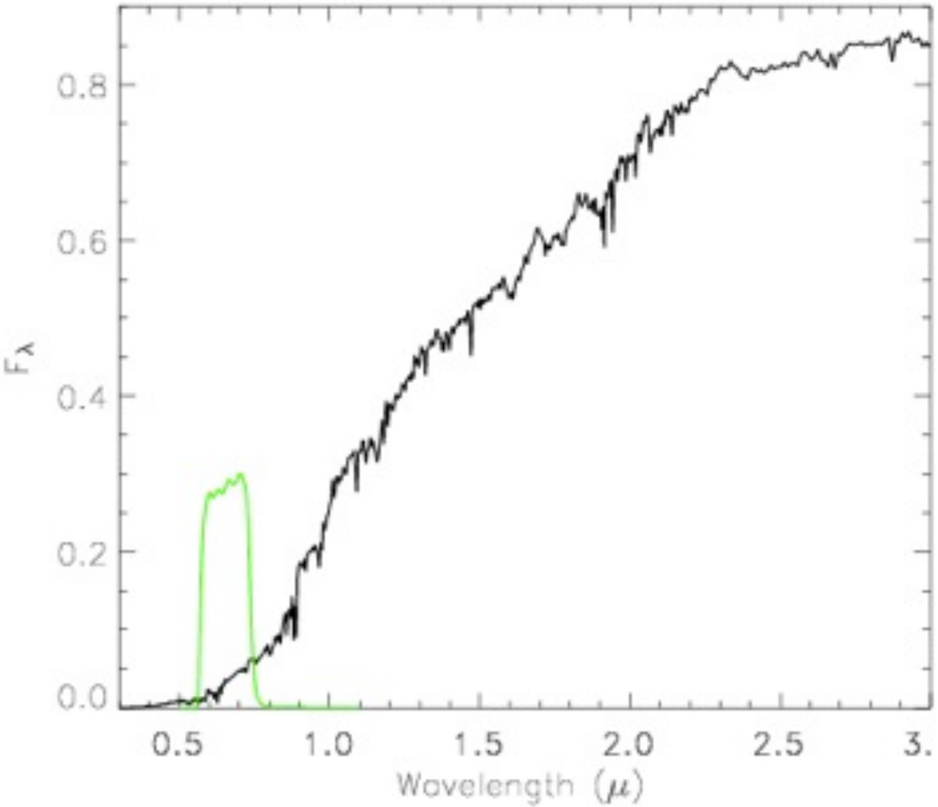

RDCS1252-29 @z=1.24 (Rosati et al.04)

Distant clusters: blue/nearIR contrast

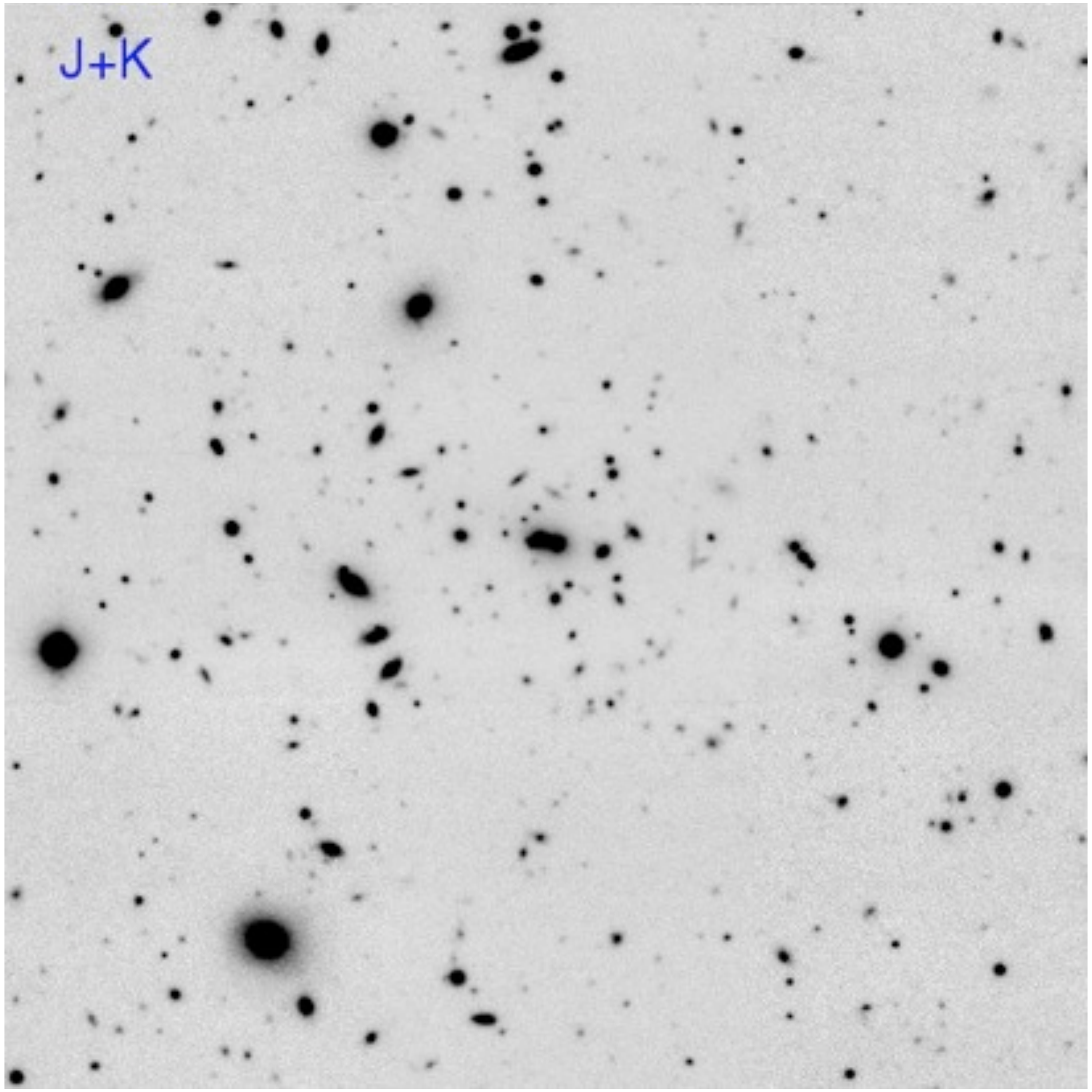

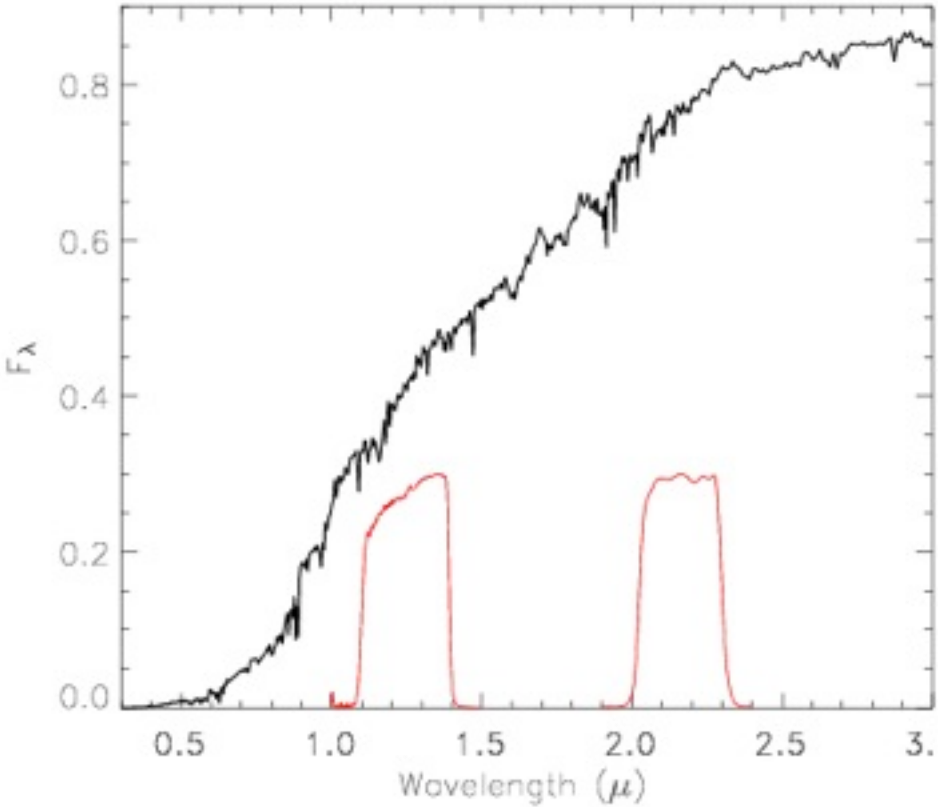

RDCS1252-29 @z=1.24 (Rosati et al.04)

Distant clusters: blue/nearIR contrast

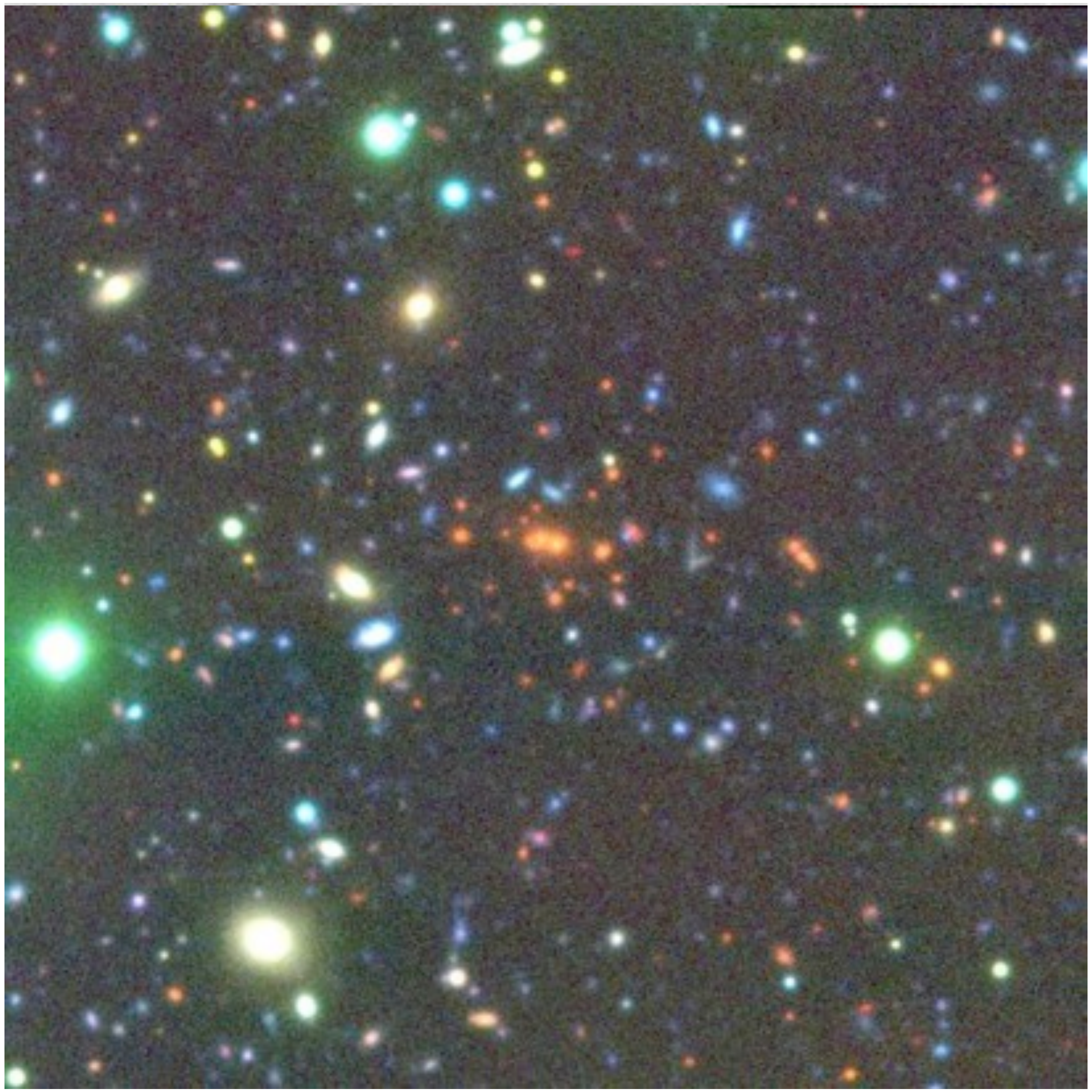

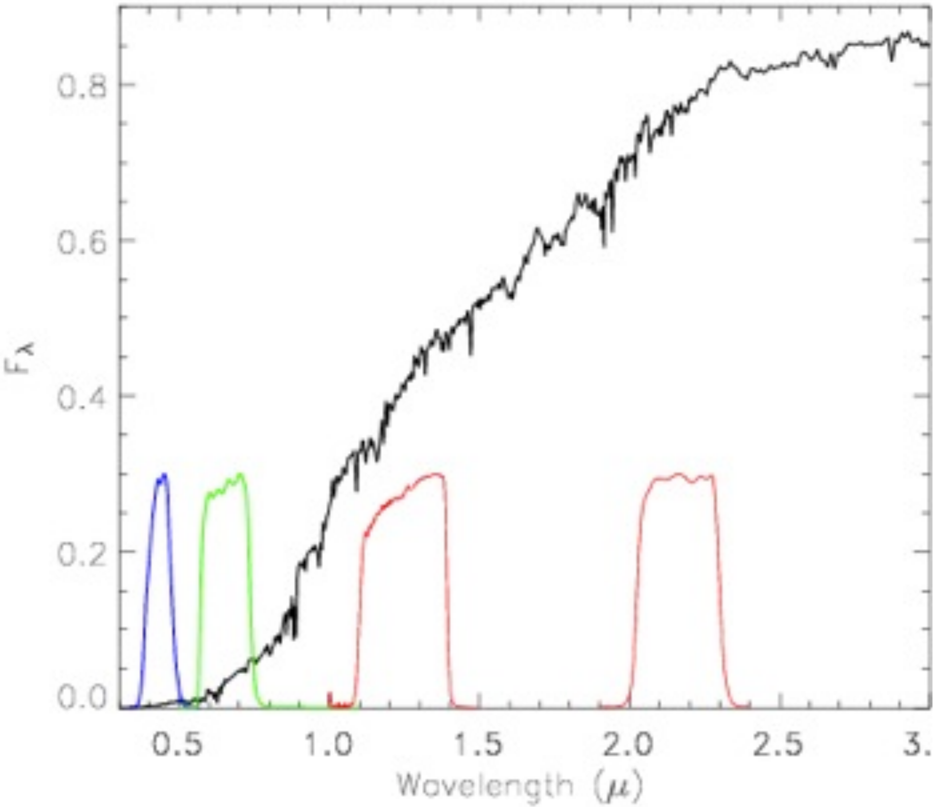

RDCS1252-29 @z=1.24 (Rosati et al.04)

Distant clusters: multi-band observations

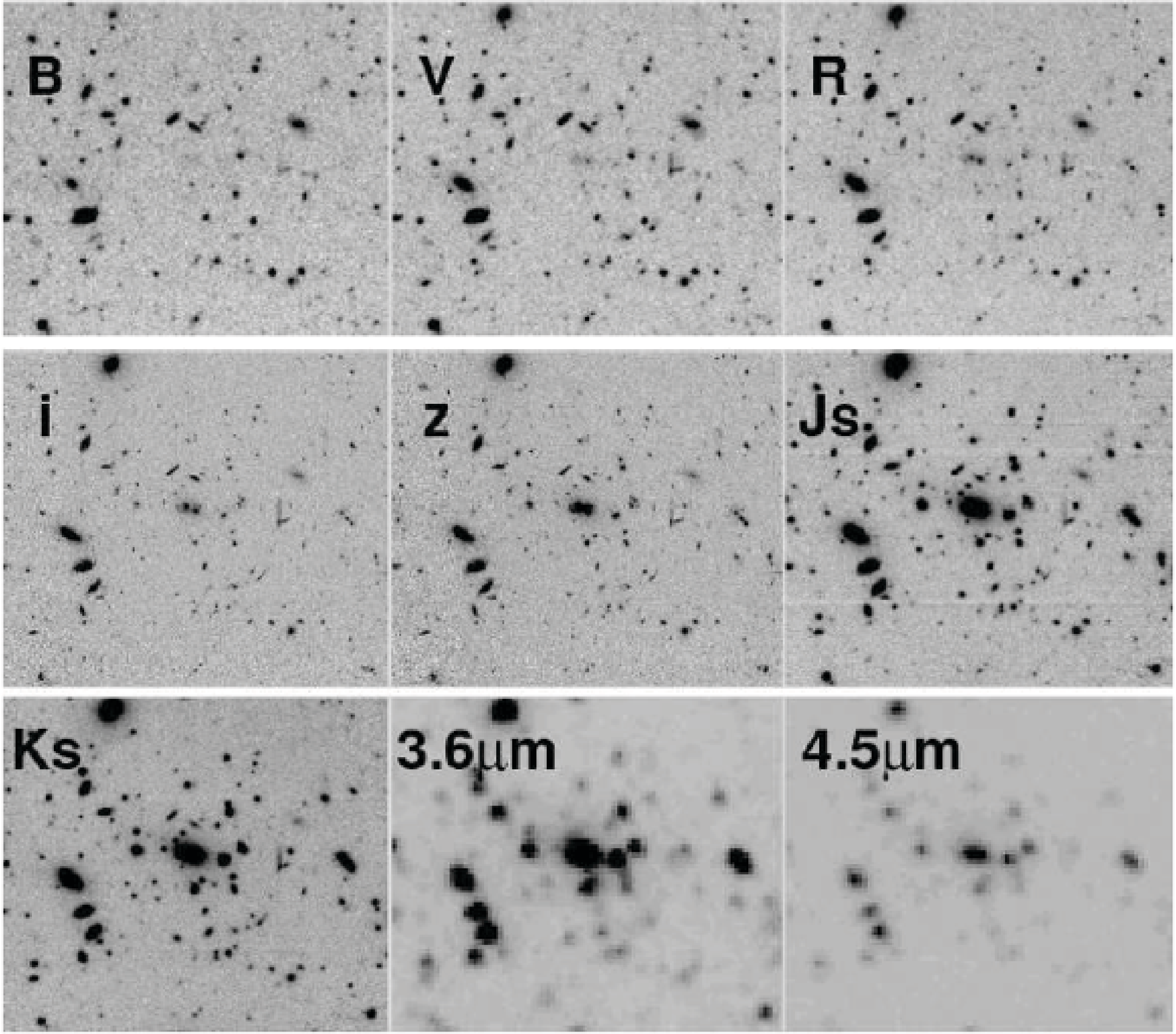

RDCS1252-29 @z=1.24

Distant clusters: multi-band observations

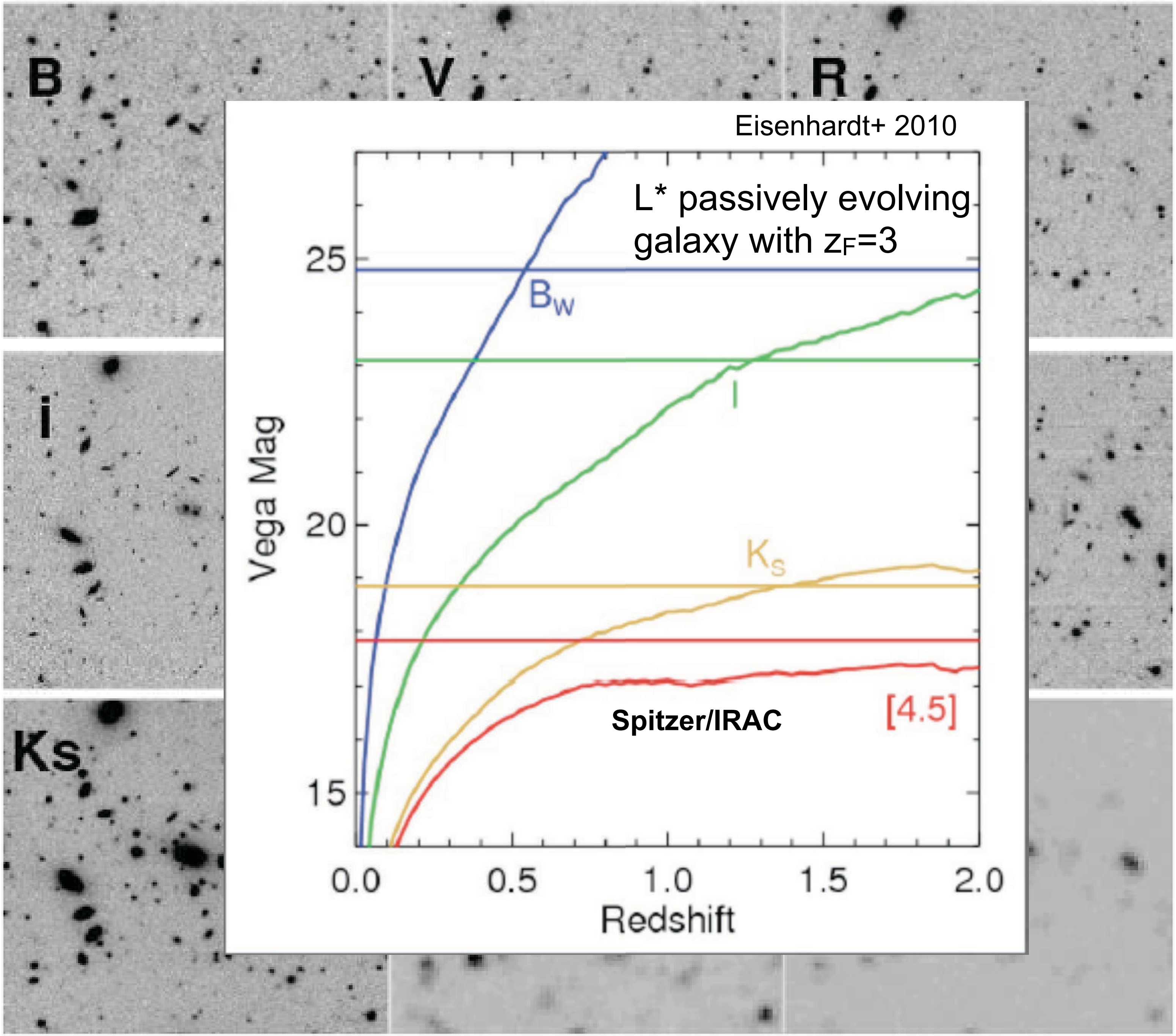

RDCS1252-29 @z=1.24

The importance to use near-IR at high z

The importance to use near-IR at high z

Brodwin et al. (2006)

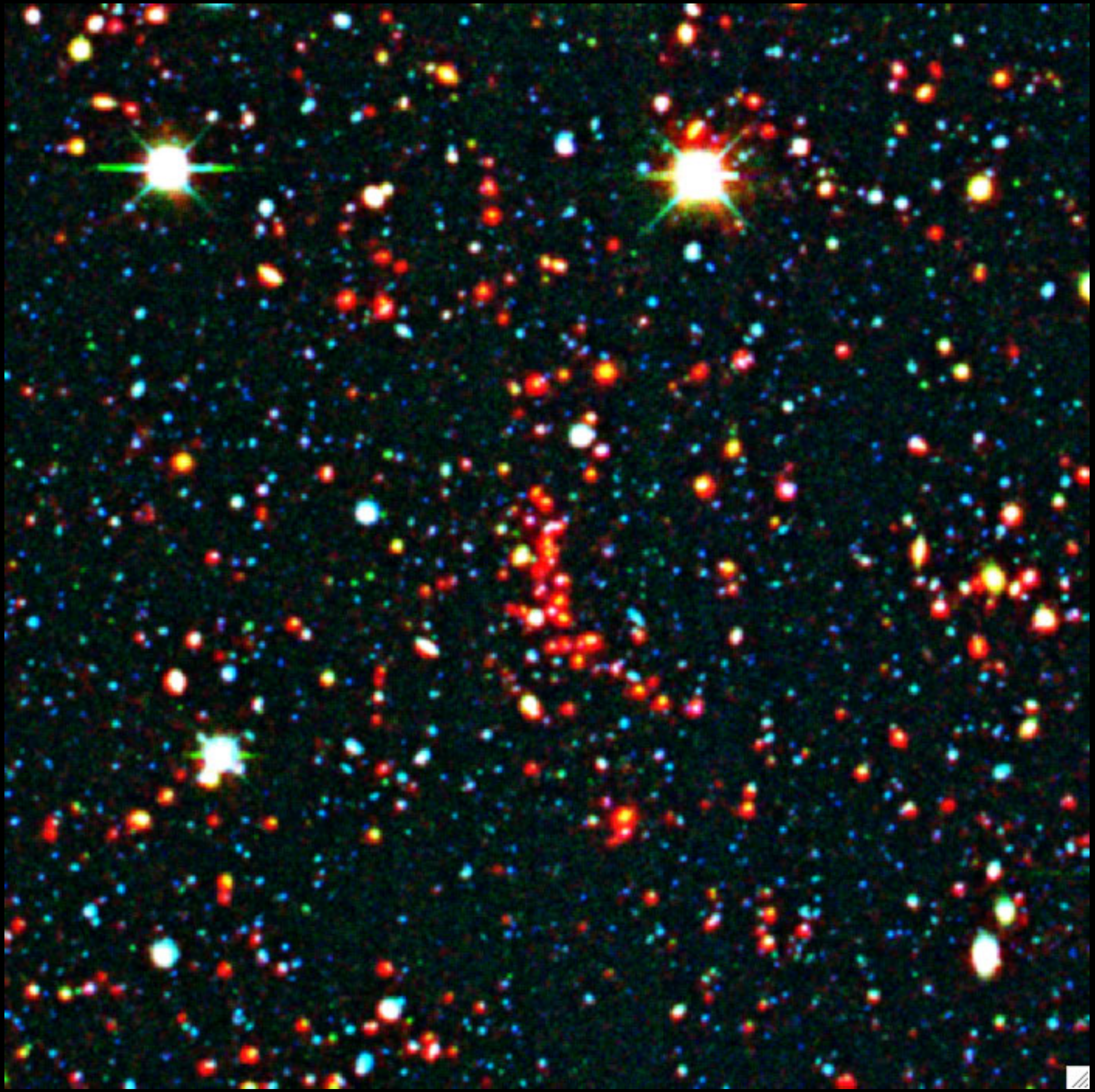

<z> = 1.243

X-ray Selected Clusters

- Uhuru satellite (1972): first X-ray all-sky survey
  - Revealed association between Abell clusters and luminous X-ray sources
  - Thermal nature of X-ray emission + Fe lines confirmed with X-ray spectra HEAO-1 A2 (1982)
- HEAO-1 satellite (1979): all-sky survey with much improved sensitivity
  - 30 out of 61 extra-gal sources identified as clusters (mostly Abell)
  - First flux-limited sample of clusters and estimate of local XLF
  - Sample further extended and improved using Ariel V and EXOSAT data (Edge et al. 90: 55 clusters, F_{lim}~1e^{-11} erg/cm^2/s)
- Einstein observatory with imaging X-ray optics opens a new era in X-ray astronomy (resolution <1′, higher sensitivity)
  - **EMSS Cluster sample** (Gioia et al. 1990): 93 clusters from 700 deg^2 with F_{lim}~1e^{-13} erg/cm^2/s : first solid assessment of cluster evolution
- ROSAT satellite (1990-2000): great advances in cluster surveys
  - Higher sensitivity, low background, resolution~30″
  - **All-sky survey** (RASS): ~1000 clusters (BCS, NORAS, REFLEX), F_{lim}~1e^{-13}
  - **Serendipitous surveys**: (RDCS, WARPS, 160 deg^2, etc..) >~200 clusters with F_{lim}~10^{-14} erg/cm^2/s
  - Together have provided the best assessment of the cluster abundance in the redshift range: 0 to 1

X-ray Selected Clusters: advantages of X-ray selection

- Physically bound systems are selected (potential wells)
- L_x well correlated with the cluster mass
- Emissivity $\propto\rho^2$, more concentrated than optical gal distribution, since X-ray sources surf. density is low $\Rightarrow$ clusters are high contrast objects in the X-ray sky
- Flux-limited samples can be defined $\Rightarrow$ search volume is known (i.e. selection function is easy to model)
- Caveats: surface brightness effects
- Limitation:
  surface brightness dimming at high-z
  difficult to cover large areas..

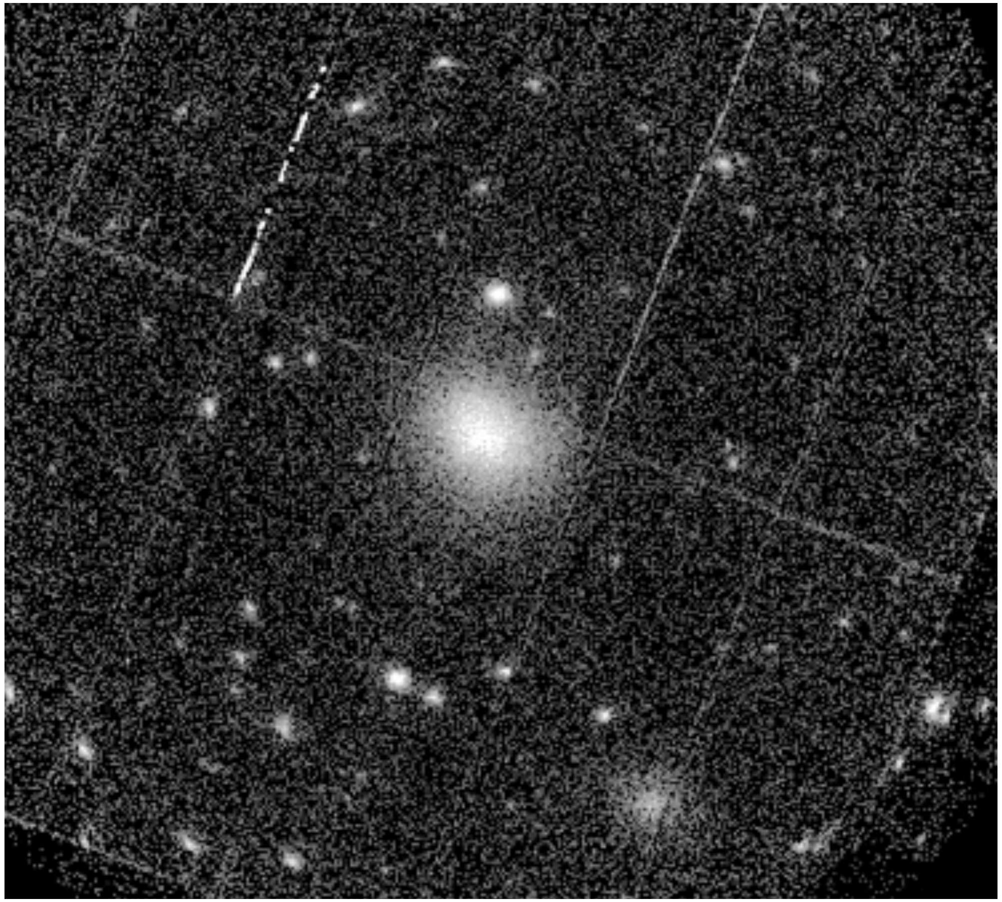

CL0016+16 and companion at z=0.58 with XMM

(Worrall & Birkinshaw 2003)

X-ray Properties

- Gas particles and galaxies are thermalized in the cluster potential well, the gas temperature:

$$k_B T \simeq \mu m_p \sigma_v^2 \simeq 6 \left(\frac{\sigma_v}{10^3\,\mathrm{km/s}} \right)^2 \mathrm{keV} = \left(\frac{\sigma_v}{10^3\,\mathrm{km/s}} \right)^2 7 \cdot 10^7\,\mathrm{K}$$

The ICM behaves as a fully ionized plasma whose emissivity is dominated by thermal bremsstrahlung (free-free collisions of free electrons with ions):

$$\epsilon_\nu \equiv \frac{dL}{dV\,d\nu} \propto n_e n_i Z^2 g(\nu, T, Z)\, T^{-1/2} \exp(-h\nu/k_B T)$$

g: Gaunt factor, n_e, n_i the number densities of electrons and ions of charge Z

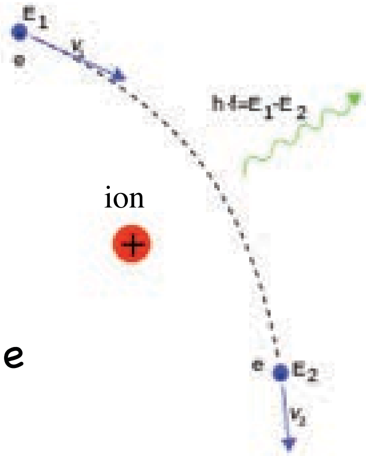

At T<~3 keV emission from collisionally excited lines contribute significantly to the emissivity (highly ionized metals, like Fe, O, Si).

X-ray spectra of clusters can be computed with collisional ionization codes (e.g. Raymond&Smith 1977) which determine the relative abundance of each ion (contribution to continuum + line emission)

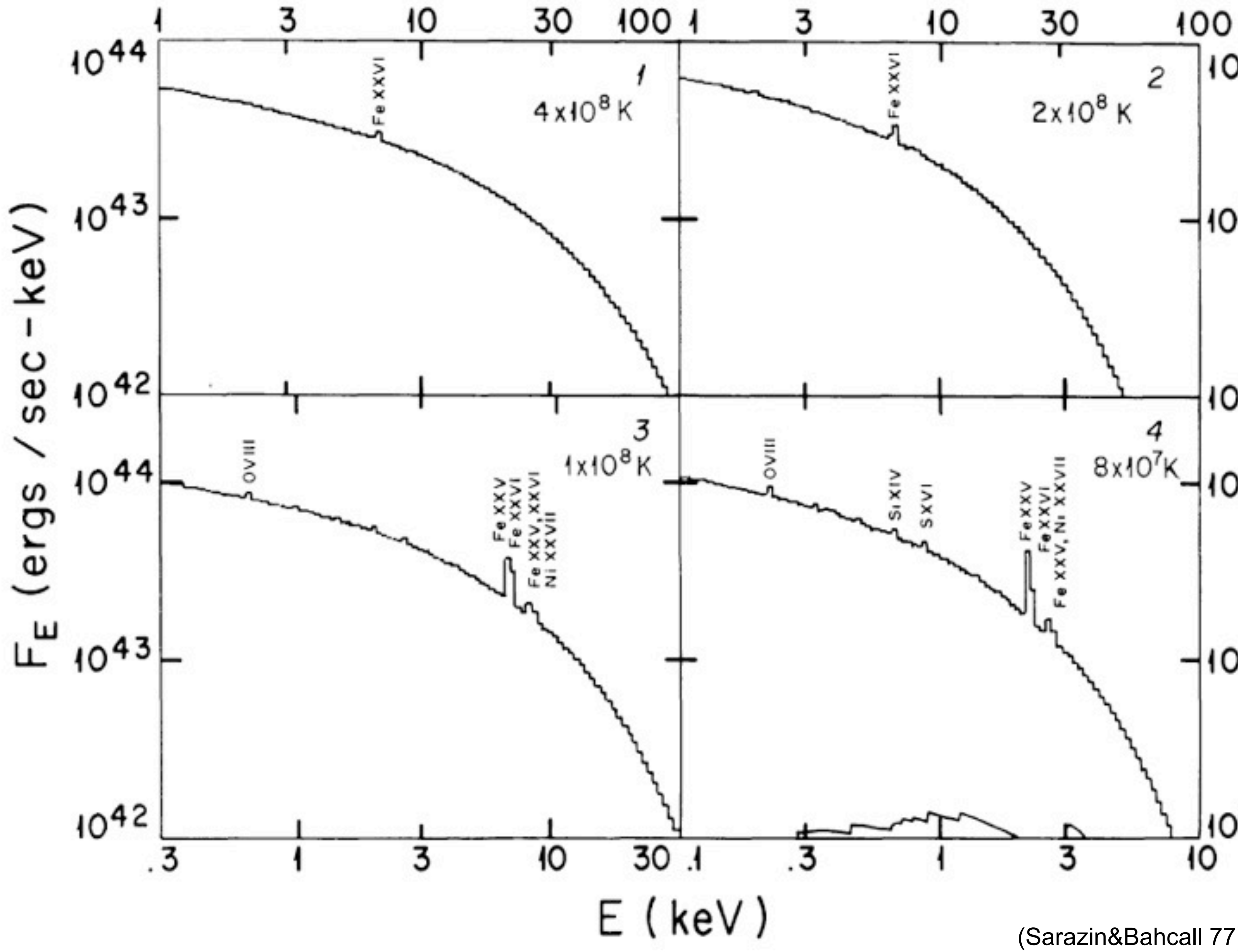

(Sarazin&Bahcall 77)

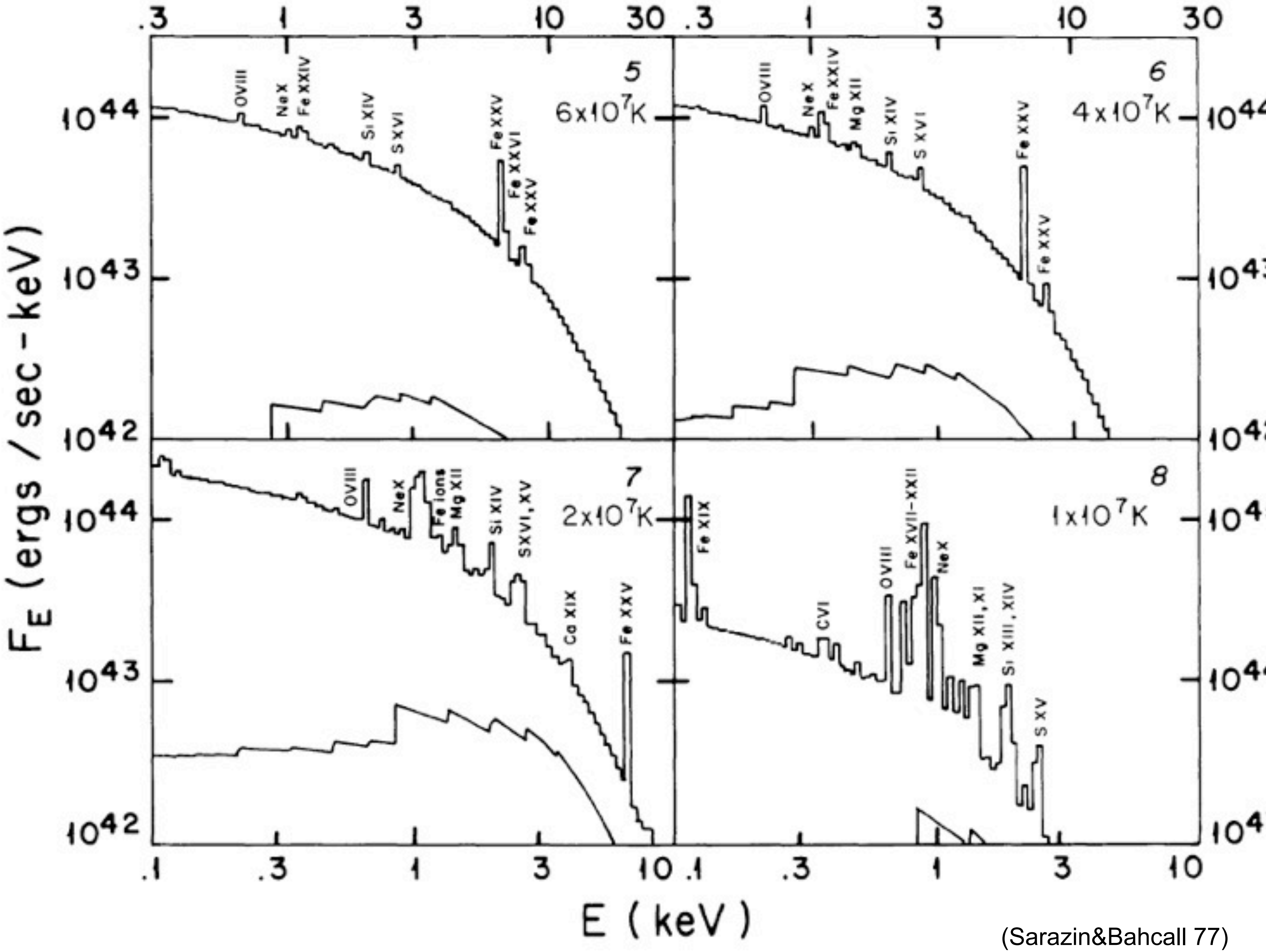

(Sarazin&Bahcall 77)

X-ray Properties

- Gas particles and galaxies are thermalized in the cluster potential well, the gas temperature:

$$k_B T \simeq \mu m_p \sigma_v^2 \simeq 6 \left(\frac{\sigma_v}{10^3\,\mathrm{km/s}}\right)^2 \mathrm{keV} = \left(\frac{\sigma_v}{10^3\,\mathrm{km/s}}\right)^2 7 \cdot 10^7\,\mathrm{K}$$

The ICM behaves as a fully ionized plasma whose emissivity is dominated by thermal bremsstrahlung (free-free collisions of free electrons with ions):

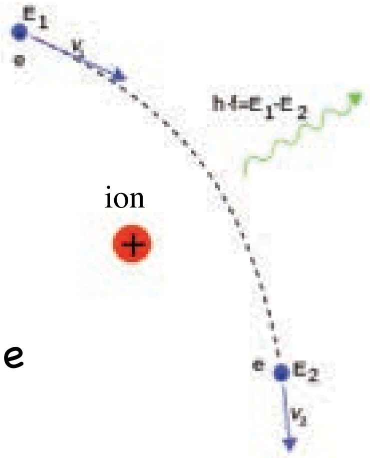

$$\epsilon_\nu \equiv \frac{dL}{dV\,d\nu} \propto n_e n_i Z^2 g(\nu, T, Z)\, T^{-1/2} \exp(-h\nu/k_B T)$$

g: Gaunt factor, n_e, n_i the number densities of electrons and ions of charge Z

At T<~3 keV emission from collisionally excited lines contribute significantly to the emissivity (highly ionized metals, like Fe, O, Si).

X-ray spectra of clusters can be computed with collisional ionization codes (e.g. Raymond&Smith 1977) which determine the relative abundance of each ion (contribution to continuum + line emission)

- The total **X-ray luminosty** of a cluster is obtained by integrating ε_ν over the energy, gas density distribution and cluster volume (➔ exercise):

$$n_p = n_0[1 + (r/r_c)^2]^{-3/2\beta}$$

$$\epsilon = 3 \times 10^{-27} \sqrt{T} n_p^2\, \mathrm{erg/cm^3/s}$$

bolometric Bremsstrahlung emissivity

$$L_X = \int \epsilon\, dV = 4.2 \cdot 10^{44} \left(\frac{T}{6\,\mathrm{kev}}\right)^{1/2} \left(\frac{n_0}{2 \cdot 10^{-3}\,\mathrm{cm}^{-3}}\right)^2 \left(\frac{r_c}{0.25\,\mathrm{Mpc}}\right)^3 \mathrm{erg/s}$$

➔ $L_X = 10^{43} - 10^{45}$ erg s^{-1} (powerful sources in the X-ray sky)

Hydrostatic equilibrium (for the gas)

Balance of gravitational and pressure forces

$$\nabla P_{gas} = -\rho_{gas} \nabla \Phi$$ $\Phi(r) = -\frac{GM}{r}$: gravitational potential

For spherical symmetry ⇒ $$\frac{dP}{dr} = -\rho_{gas}\frac{d\Phi}{dr} = -\rho_{gas}\frac{GM(r)}{r^2}$$

with $p = \rho_{gas} k_B T/\mu m_p$ ➪ $$\frac{d\,ln\rho_g}{dr} = -\frac{\mu m_p}{k_B T}\frac{d\phi(r)}{dr}$$

$$M(<r) = -\frac{r^2}{G\rho_{gas}}\frac{dP}{dr} = \frac{r}{G}\frac{kT}{\mu m_p}[\frac{d\ln\rho_{gas}}{d\ln r} + \frac{d\ln T}{d\ln r}]$$

If the potential comes from by a King dark-matter density profile, $\rho(r) = \rho_0[1+(r/r_c)^2]^{-3/2}$, then an isothermal gas in hydrostatic equilibrium follows the "β model" (➔ exercise):

$$\rho_g(r) = \rho_{g,0}\left[1 + \left(\frac{r}{r_c}\right)^2\right]^{-3\beta/2},$$ with core radius r_c and $\beta \equiv \frac{\mu m_p \sigma_r^2}{k_B T}$

Hydrostatic equilibrium (for DM and galaxies)

For a collisionless system of particles (CDM, galaxies) the equilibrium condition is given by the Jeans equation, which for a non-rotating spherically symmetric system, is:

$$M_J(< r) = -\frac{r\sigma_r^2}{G}\left[\frac{d\ln \overset{\substack{\text{density profile}\\ \downarrow}}{\nu}(r)}{d\ln r} + \frac{d\ln \overset{\substack{\text{radial vel.dispersion profile}\\ \downarrow}}{\sigma_r}(r)^2}{d\ln r} + 2\underset{\substack{\uparrow\\ \text{anisotropy profile}}}{\beta}(r)\right]$$

$\beta = 1 - \frac{\sigma_t^2}{2\sigma_r^2}$ is the orbit anisotropy parameter (β=0 for isotropic velocity field) in terms of radial and tangential vel. disp. components

The observed quantities: projected density profile N(R) and line of sight vel.dispersion profile, $\sigma_{los}(r)$, need to be deprojected with Abell integrals, e.g. $\nu(r) = -\frac{1}{\pi}\int_r^\infty \frac{dN}{dR}\frac{dR}{\sqrt{R^2 - r^2}},$

Different combinations of M(r) and β(r) can give the same N(R) and $\sigma_{los}(r)$, this is the so-called “mass-anisotropy degeneracy“ which can be removed with higher order moments of the velocity distribution, or simply with an independent knowledge of M(r)

Observations show a small deviation from $\sigma_r \sim T^{1/2}$ (if both quantities were to track cluster mass), but rather $\sigma_r \sim T^{\sim 0.6}$, implying β=0.97 at 6 keV

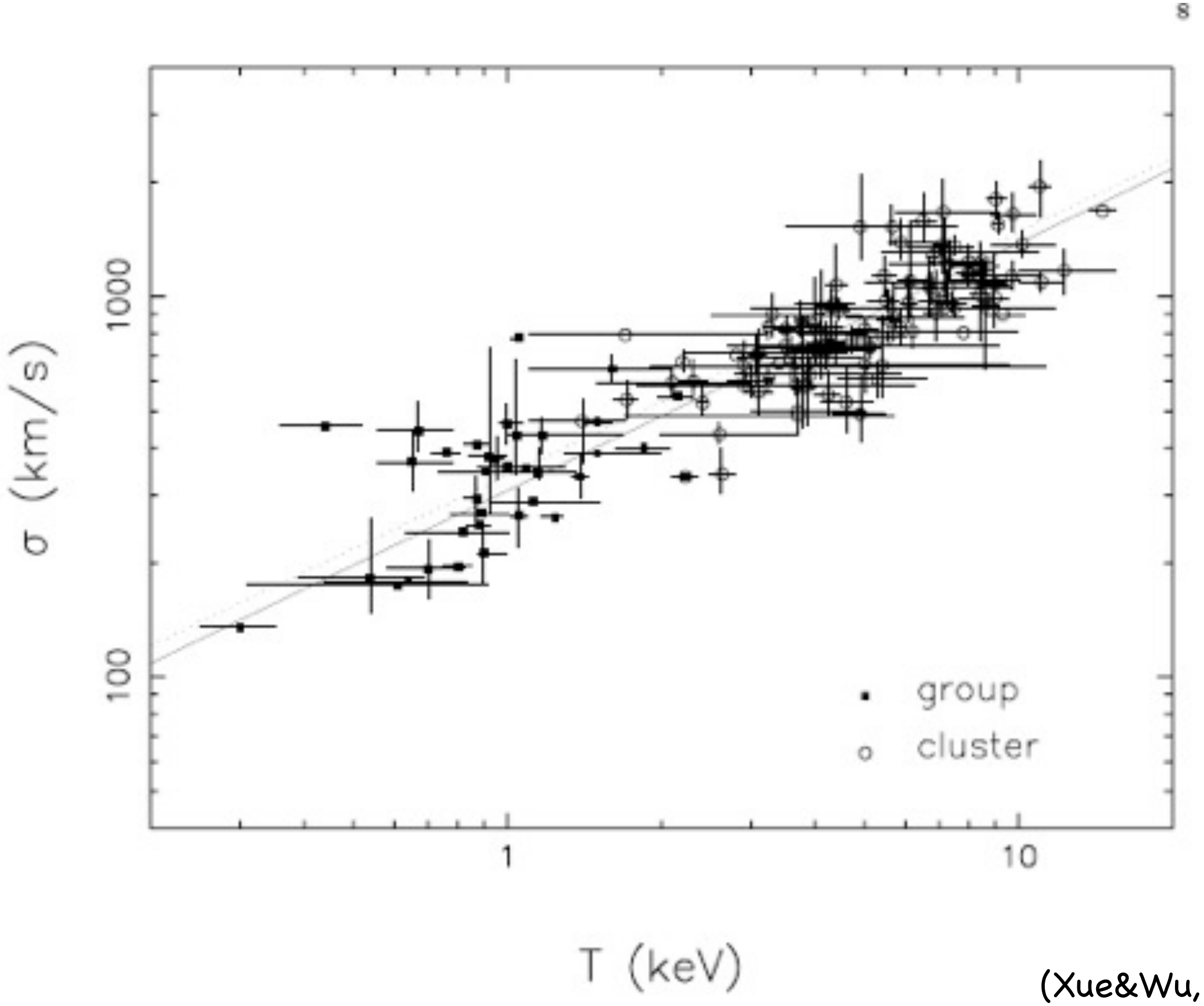

(Xue&Wu, 2000)

Total gravitating mass:

plugging the β-profile in the hydrostatic equilibrium equation (with T=const):

$$\boxed{M(<r) = \frac{3\beta k_B T}{G\mu m_p}\frac{x^2}{1+x^2}r\,, \quad \text{with} \quad x = r/r_c}$$

$$= (10^{14} M_\odot)\,\beta\,k_B T(\text{keV})\frac{x^2}{1+x^2}\,r(\text{Mpc})$$

For x>>1, and β=2/3 one finds the expression for the SIS

When a spatially resolved temperature is available, a polytropic law is often used, so $p \sim \rho_g^\gamma \rightarrow T(r) \sim \rho_g^{\gamma-1}$ and:

$$\boxed{M(<r) = r\,\frac{3\beta\gamma k_B T(r)}{G\mu m_p}\,\frac{x^2}{1+x^2}}$$

Projected surface brigthness (flux per unit solid angle):

The Surface Brightness at freq. ν and at projected distance b from the center of a spherical cluster is:

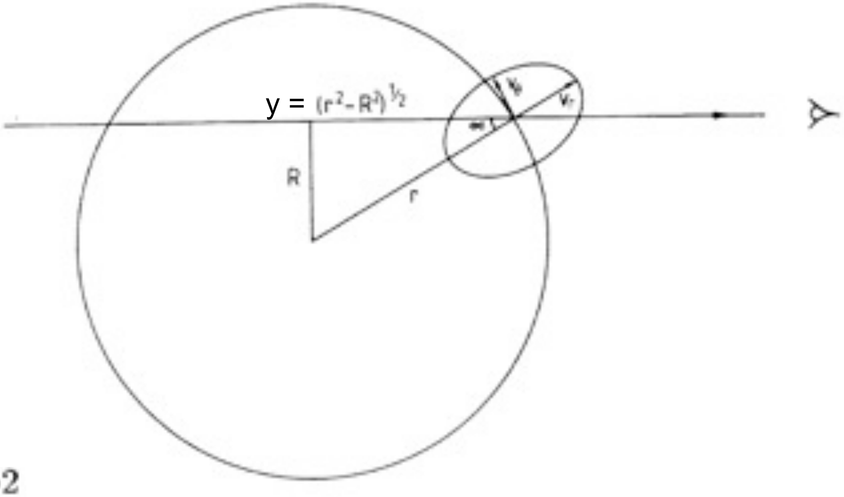

$$I_\nu(R) = \int \epsilon_\nu(r)dy = \int_{R^2}^{\infty} \frac{\epsilon_\nu(r)dr^2}{\sqrt{r^2 - R^2}}$$

where ε_ν is the emissivity $\epsilon_\nu = n_e^2 \Lambda_\nu(T)$

The Abell integral can be inverted to infer ε_ν(r):

$$\epsilon_\nu = -\frac{1}{2\pi r}\frac{d}{dr}\int_{r^2}^{\infty} \frac{I_\nu(R)dR^2}{\sqrt{R^2 - r^2}}$$

Assuming β-model for the gas density, the SB function to fit to the cluster X-ray image is: (➔ exercise)

$$S_X(R) = S_0 \left(1 + \frac{R^2}{r_c^2}\right)^{-3\beta+1/2} + B$$

But note:

$$S_X = \frac{F_X}{\pi\Theta^2} = \frac{L_X}{4\pi D_L^2} \cdot \frac{D_A^2}{\pi d^2} \propto \boxed{(1+z)^{-4}}$$

The gas mass is simply:

$$M_{gas}(<R) = 4\pi \int_0^R \rho(r) r^2 dr = 4\pi \rho_0 r_c^3 \int_0^{r/r_c} (1+x^2)^{-3/2\beta} x^2 dx\,, \quad x = r/r_c$$

$$M_{gas} = 4\pi \int_0^\infty \rho(r) r^2 dr = \pi^{3/2} \rho_0 r_c^3 \frac{\Gamma[3(\beta-1)/2]}{\Gamma[3\beta/2]}\,, \quad \text{for } \beta > 1$$

$$= 3.15 \times 10^{12} M_\odot \left(\frac{n_0}{10^{-3}\mathrm{cm}^{-3}}\right) \left(\frac{r_c}{0.25\,\mathrm{Mpc}}\right)^3 \frac{\Gamma[3(\beta-1)/2]}{\Gamma[3\beta/2]}$$

The gas mass fraction is: $f_{gas} = M_{gas}/M_{tot} \simeq (0.10 - 0.12) h_{70}^{-3/2}$

from a large number of observations (Mohr et al., Ettori et al., Allen et al.)

The stellar mass fraction is: $f_{stars} = M_{stars}/M_{tot} \approx 1\%$

For a cluster with 100 galaxies: $M_{\rm stars} \lesssim 100 L_* \langle \frac{m}{l} \rangle \approx 1 \times 10^{13} M_\odot$

where $L_* = (2-3) \times 10^{10} L_\odot$ from $dN/dL = (\Phi_*/L_*)(L/L_*)^{-\alpha} \exp(-L/L_*)$

$\langle \frac{m}{l} \rangle \approx 7$ typical mass-to-light ratio of evolved stellar populations

The gas mass is simply:

$M_{gas}(< R)$ … $x = r/r_c$

$M_{gas} = 4\pi \int$

$= 3.15$ … $]$

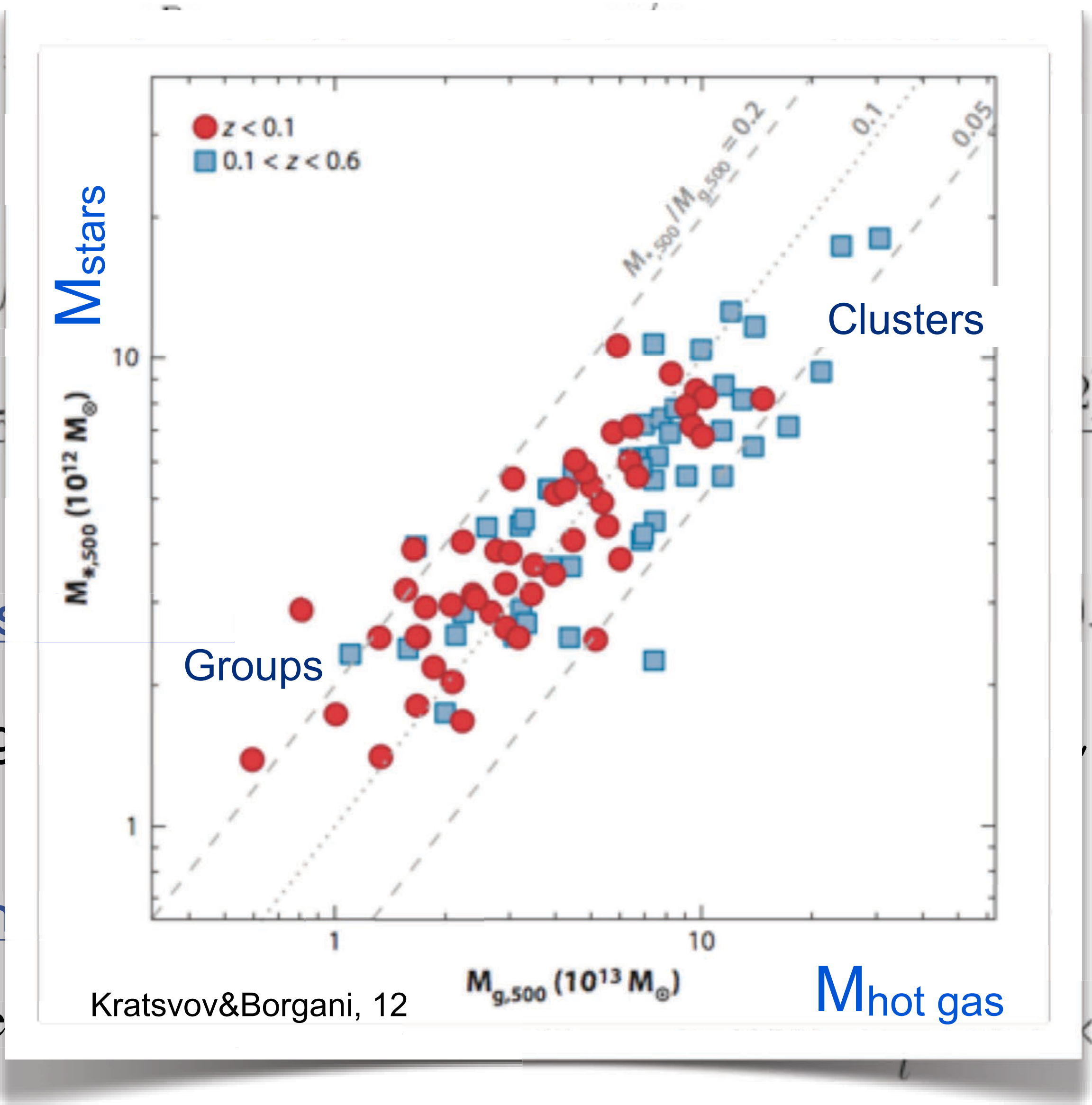

Kratsvov&Borgani, 12

The gas mass … $.12)h_{70}^{-3/2}$

from a larg … , Allen et al.)

The stellar m

For a cluste … $10^{13} M_\odot$

where $L_* = (2-3) \times 10^{10} L_\odot$ from $dN/dL = (\Phi_*/L_*)(L/L_*)^{-\alpha} \exp(-L/L_*)$

$\langle \frac{m}{l} \rangle \approx 7$ typical mass-to-light ratio of evolved stellar populations

X-ray Cluster Surveys (1980 - 2010)

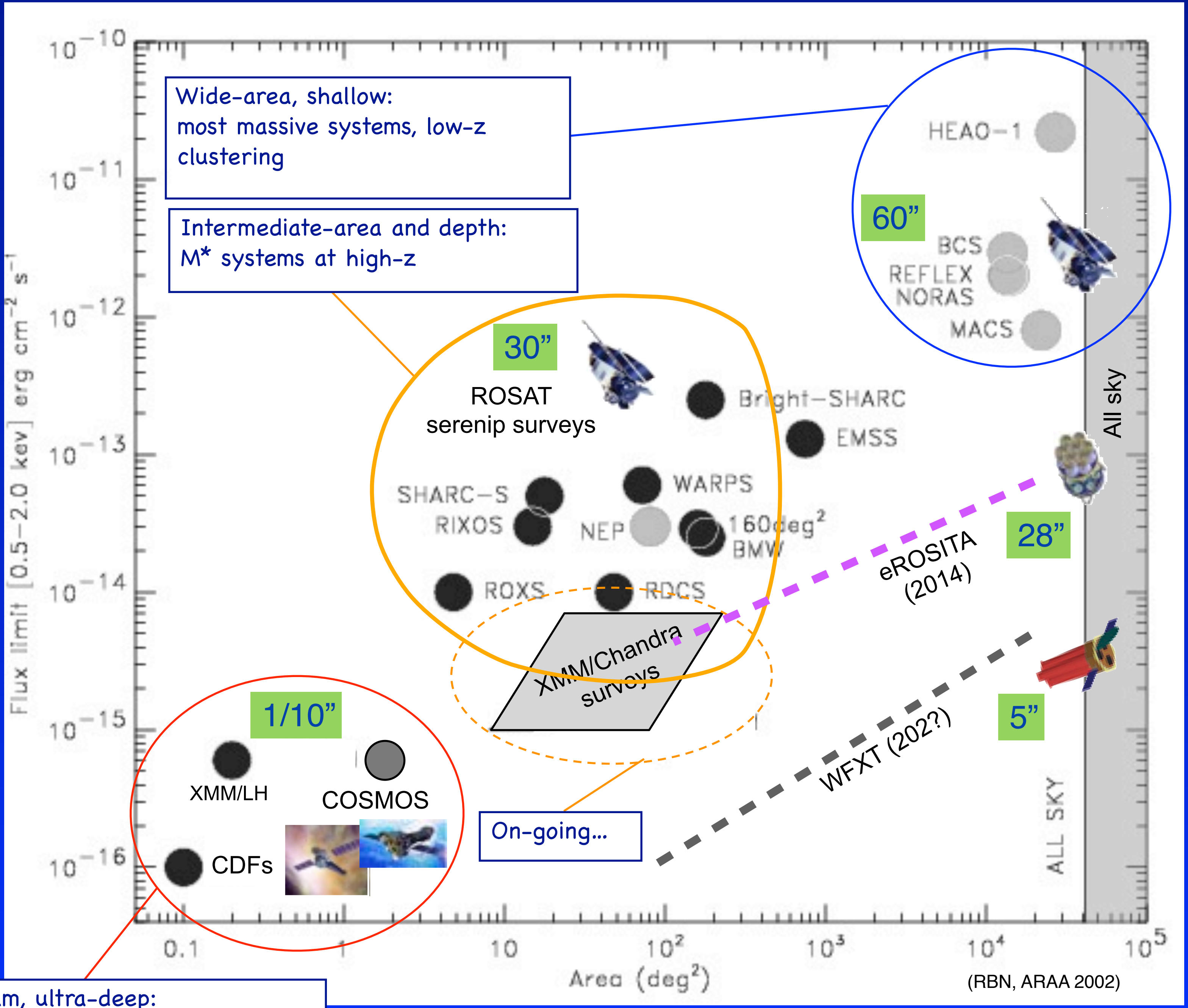

Wide-area, shallow:
most massive systems, low-z
clustering

Intermediate-area and depth:
M* systems at high-z

On-going...

Pencil-beam, ultra-deep:
less massive systems at high-z

(RBN, ARAA 2002)

Cluster searches with (Sunyaev-Zel'dovich) SZ Effect

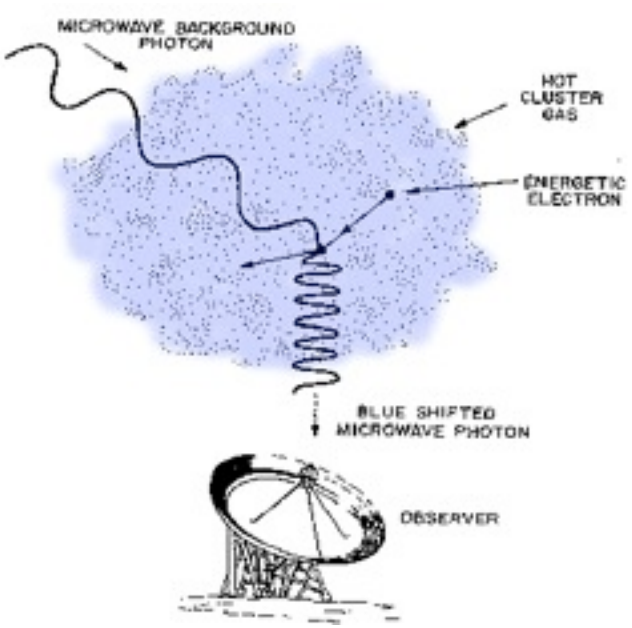

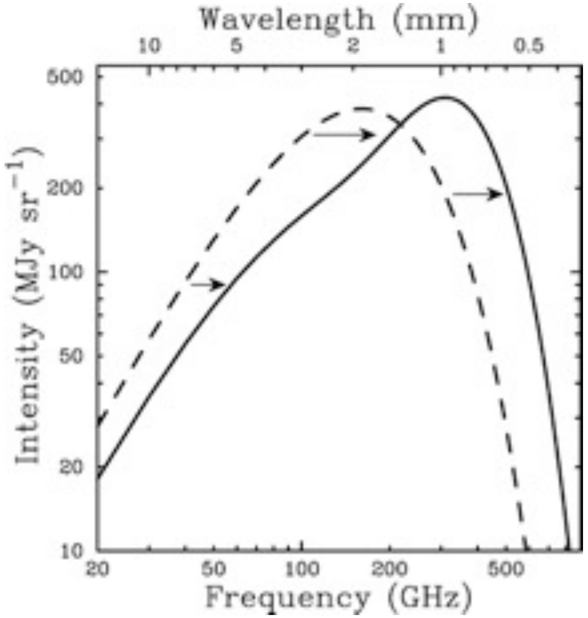

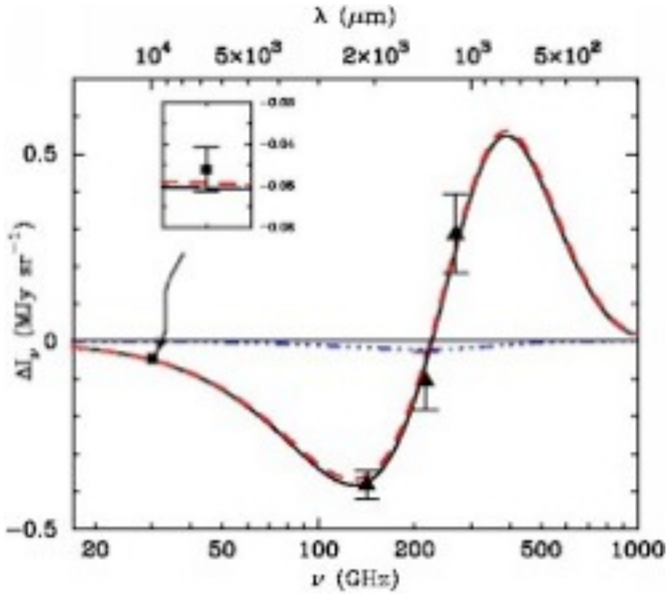

(Birkinshaw 2003)

- The SZ effects is the results of inverse-Compton scattering by hot electrons on cold CMB photons, causing a distortion of the CMB spectrum around 218 GHz (2mm)
- The principal (thermal) SZ effect has an amplitude proportional to the Comptonization parameter, y_e, the dimensionless electron temperature weighted by the scattering optical depth, i.e. the integral of the pressure along the line of sight

Distortion = freq_dependence × Amplitude: $\Delta T_{SZ}/T_{CMB}=f(\nu)\ y_e$

$$y_e = \int n_e \sigma_T \, dl \left(\frac{k_B T_e}{m_e c^2}\right) = \int d\tau_e \left(\frac{k_B T_e}{m_e c^2}\right)$$

($y \approx 10^{-4}$ for hot clusters)

Main properties of the SZ effect

- Distinct spectral signatures (from background CMB fluctuations)
- Amplitude (almost) independent of redshift ➔ powerful for finding clusters at very high-z and therefore as a cosmological tool
- Above a given z and mass the sample is basically volume complete
- The integrated SZ flux $\propto$ total thermal energy of the cluster, or the temperature-weighted mass divided by $D_A^2(z)$:

$$d\Omega = dA/D_A^2$$

$$\int \Delta_{SZ} d\Omega \propto \frac{N_{e,tot}\langle T_e\rangle}{D_A^2} \propto \frac{M\langle T_e\rangle}{D_A^2}$$

- SZ clusters have a larger angular size ($\propto\rho$, instead of $\propto\rho^2$ as in X-ray) ➔ great tools to study the outskirts of clusters (to R_{vir})

- Challenges
  - Confusion from point sources (radio-syncroton, submm/mm-dust)
  - Confusion from CMB anisotropies on large angular scales ➔ need small (~1′) beam and multi-frequencies observations
  - Signal is weak, only $M>10^{14} M_\odot$ weak are detectable with best current technologies (1-2 clusters/deg^2)
  - Relating Y to M requires to fit a scaling between the SZ S/N and M: $S/N \sim M^A H(z)^B$!

Cluster searches with SZ Effect: early work

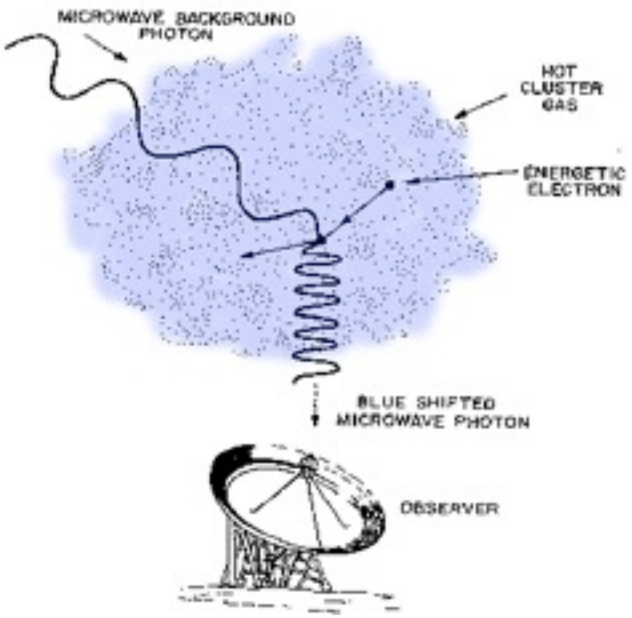

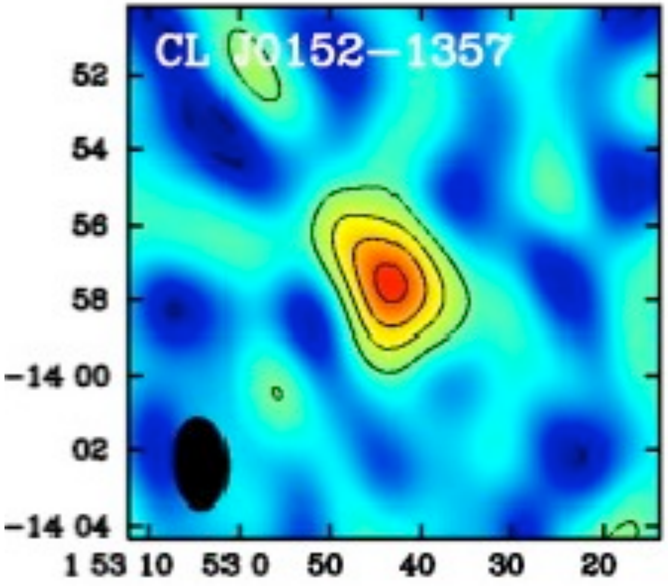

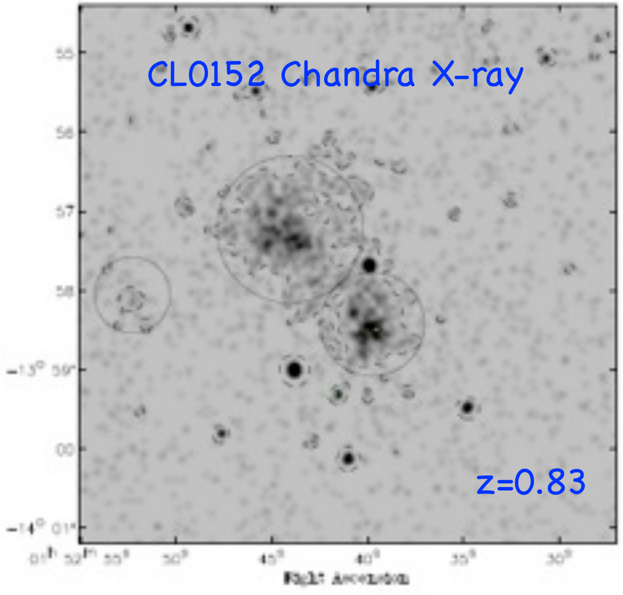

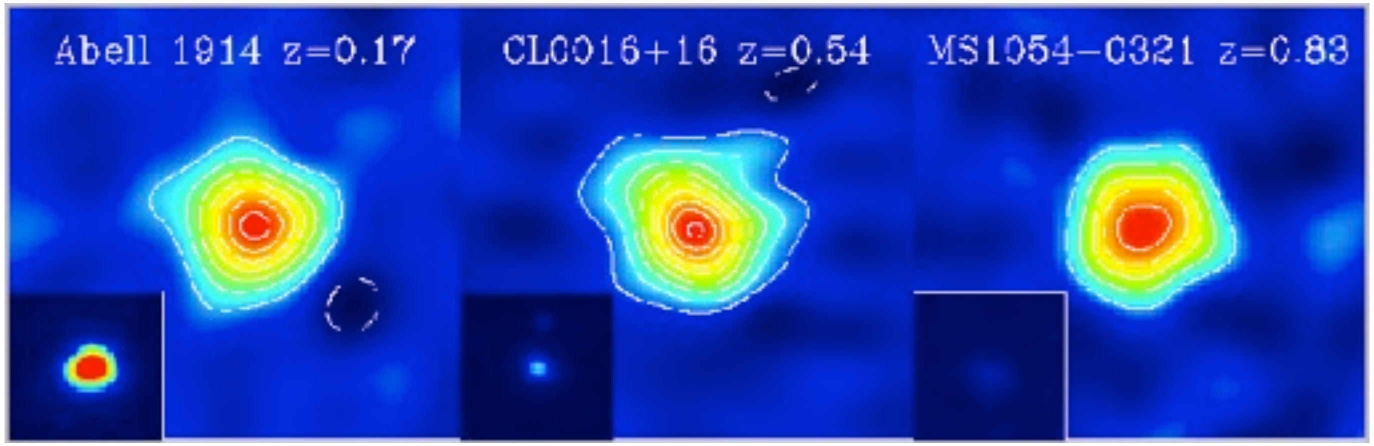

Carlstrom et al. 02
(BIMA observations)

The new era of SZ cluster surveys

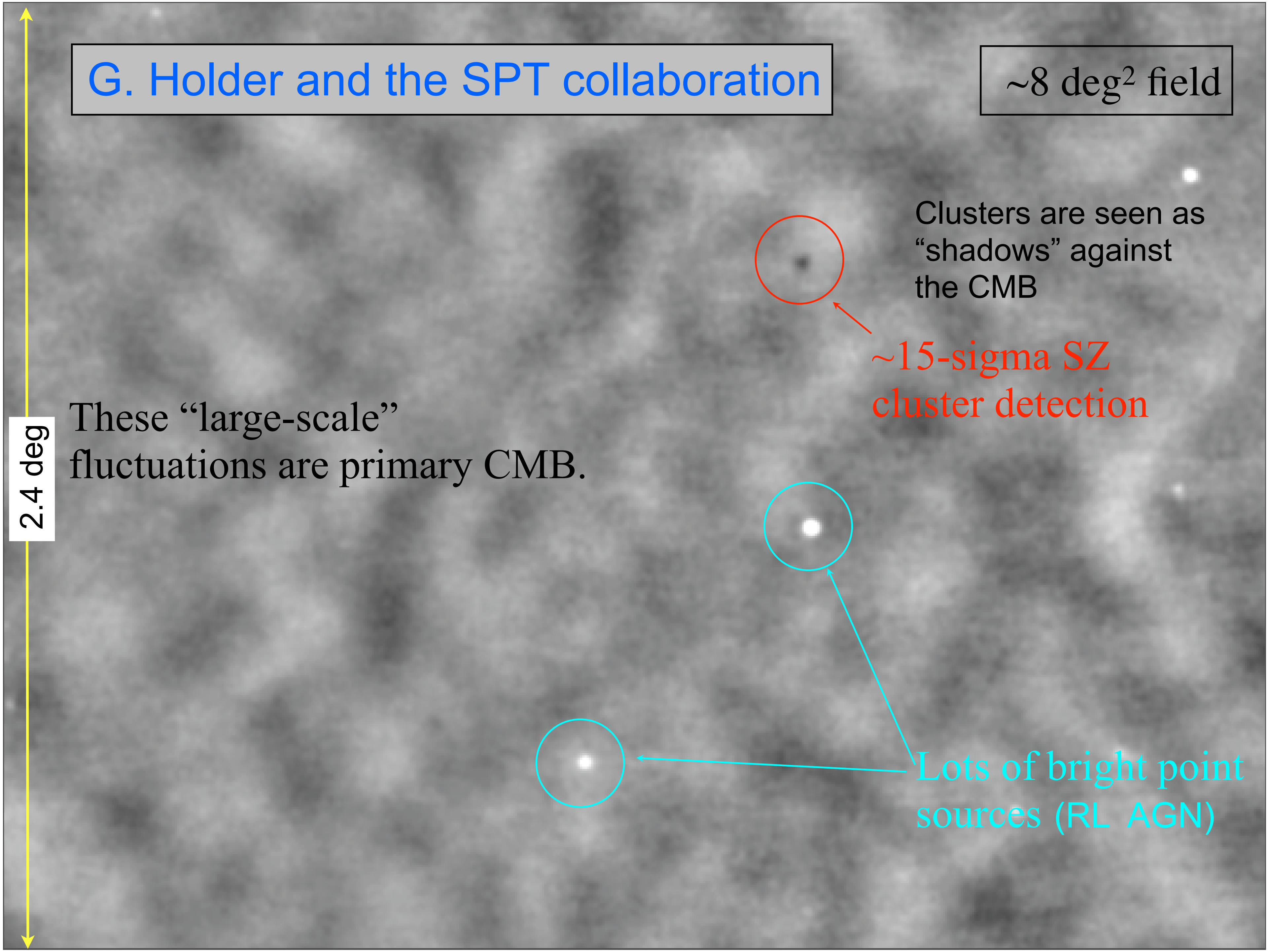

G. Holder and the SPT collaboration

~8 deg^2 field

Clusters are seen as “shadows” against the CMB

~15-sigma SZ cluster detection

These “large-scale” fluctuations are primary CMB.

Lots of bright point sources (RL AGN)

The new era of SZ cluster surveys

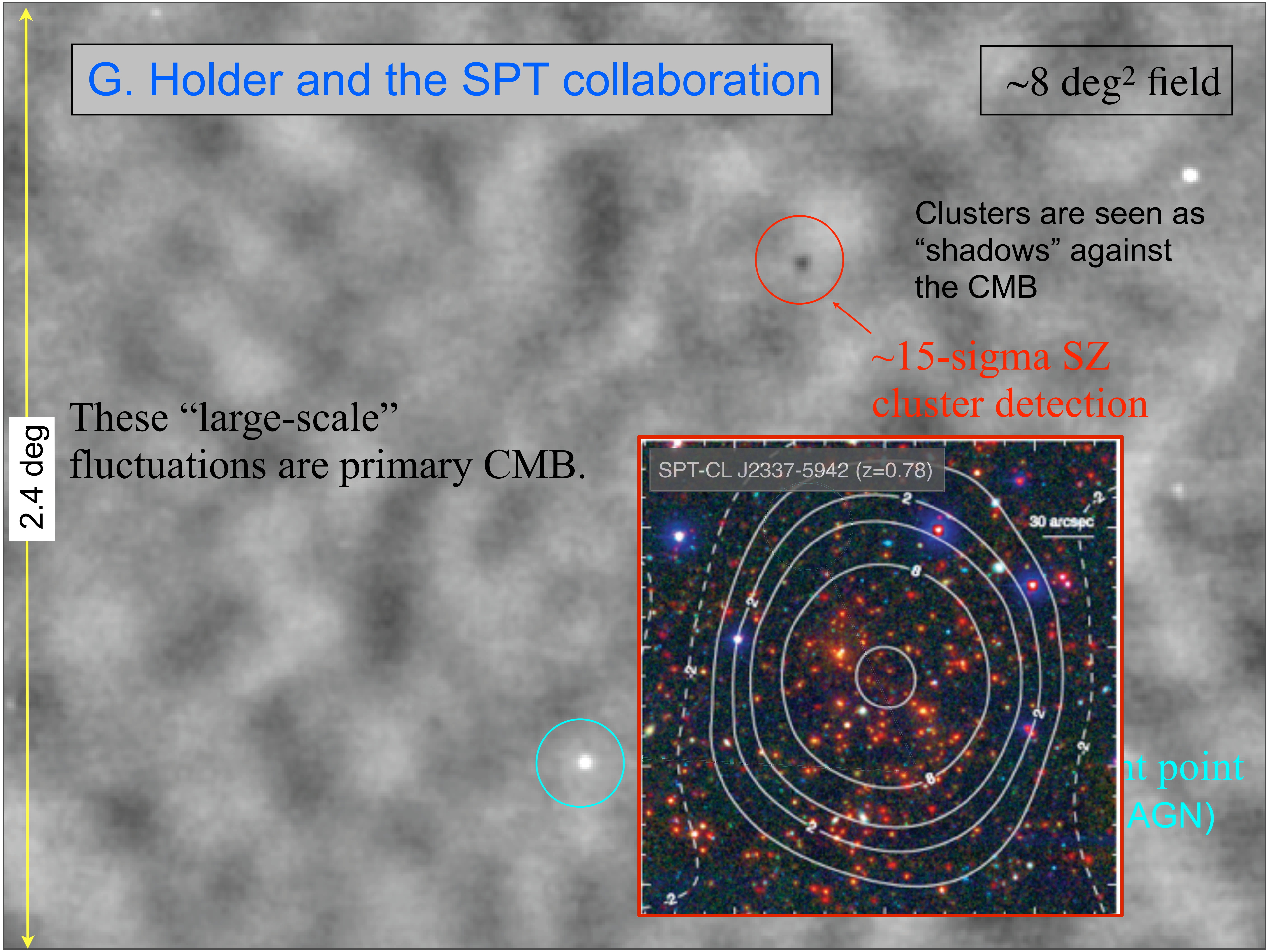

G. Holder and the SPT collaboration

~8 deg^2 field

Clusters are seen as “shadows” against the CMB

~15-sigma SZ cluster detection

These “large-scale” fluctuations are primary CMB.

t point

AGN)

Cluster searches with (Sunyaev-Zel'dovich) SZ Effect

- **Main on-going/upcoming SZ surveys**
  - **South Pole Telescope** (SPT, Carlstrom et al. Chicago-Berkeley) 4000 deg^2 survey, arcmin resolution. Status: ~90% complete
  - **Atacama Cosmology Telescope** (ACT) Survey: Princeton (Page) et al. 500 deg^2 survey, arcmin resolution. Status: nearing completion
  - **Apex** (Atacama Pathfinder EXperiment) SZ survey: Berkeley Bolom array on the Max Planck prototype ALMA 12 m ESO telescope in Atacama, 200 deg^2 survey, arcmin resolution. Status: testing

Planck Cluster sample early release (ESZ)
(Planck collaboration, ESZ)

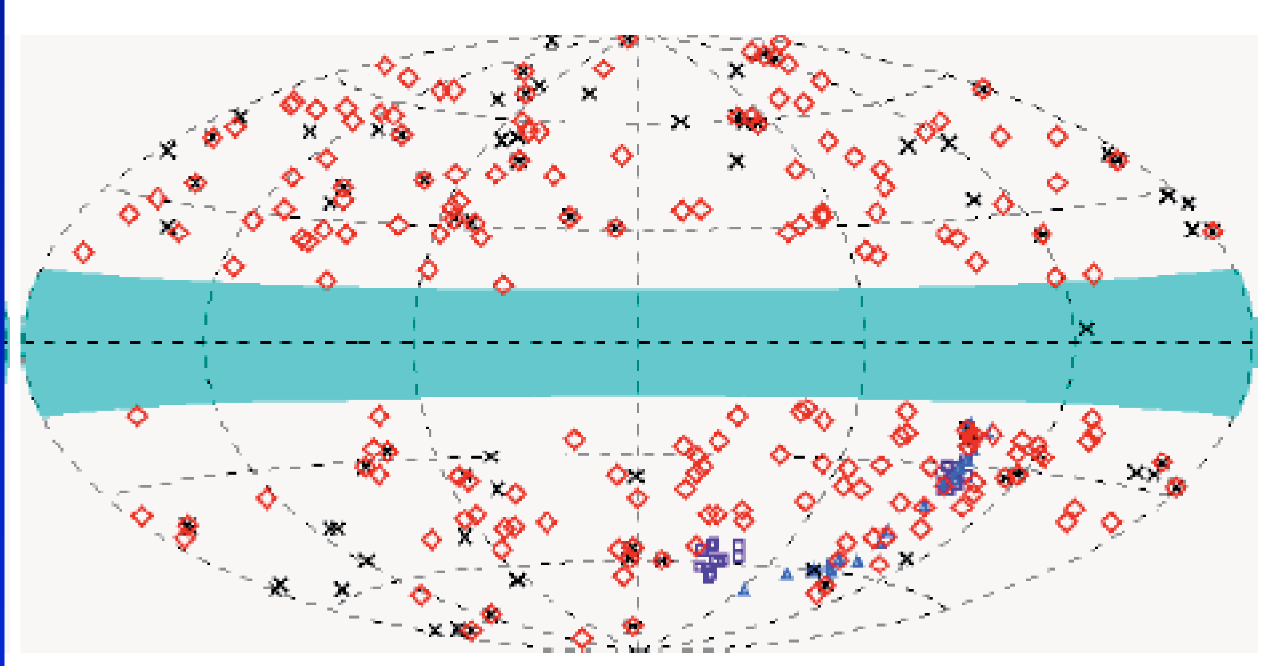

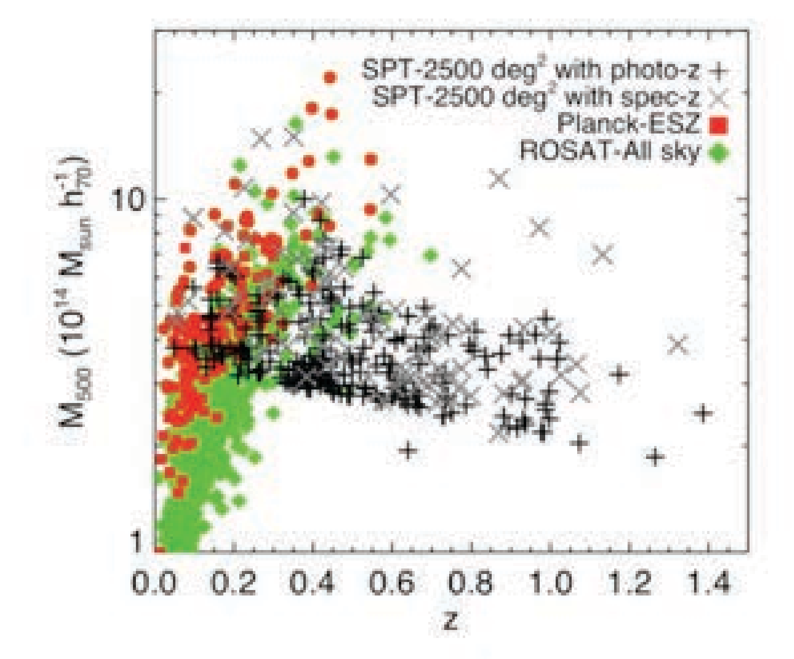

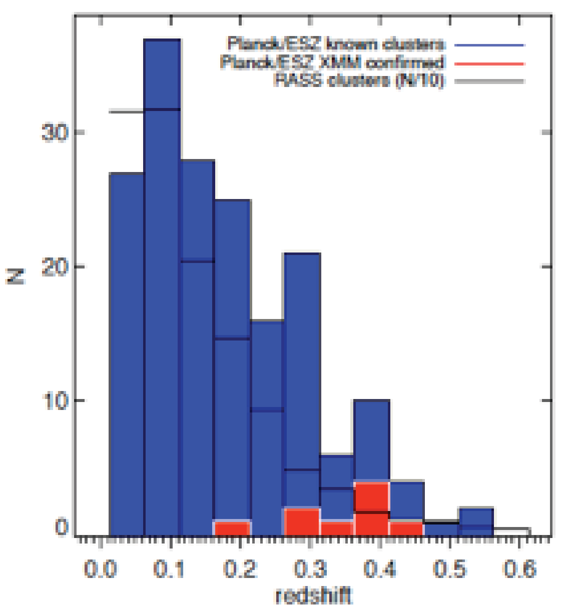

- All-sky (|b|>14 deg) SZ cluster survey (~5’ beam)
- 189 clusters (S/N>6, 6 frequencies), 20 new
- Most at z<0.3, massive (>10^{14} M☉), out to z~1
- Excellence reference low-z sample once characterized
- **Larger diversity (low-Lx, merging system) compared to X-ray sample (RASS)**

Planck Cluster sample early release (ESZ)
(Planck collaboration, ESZ)

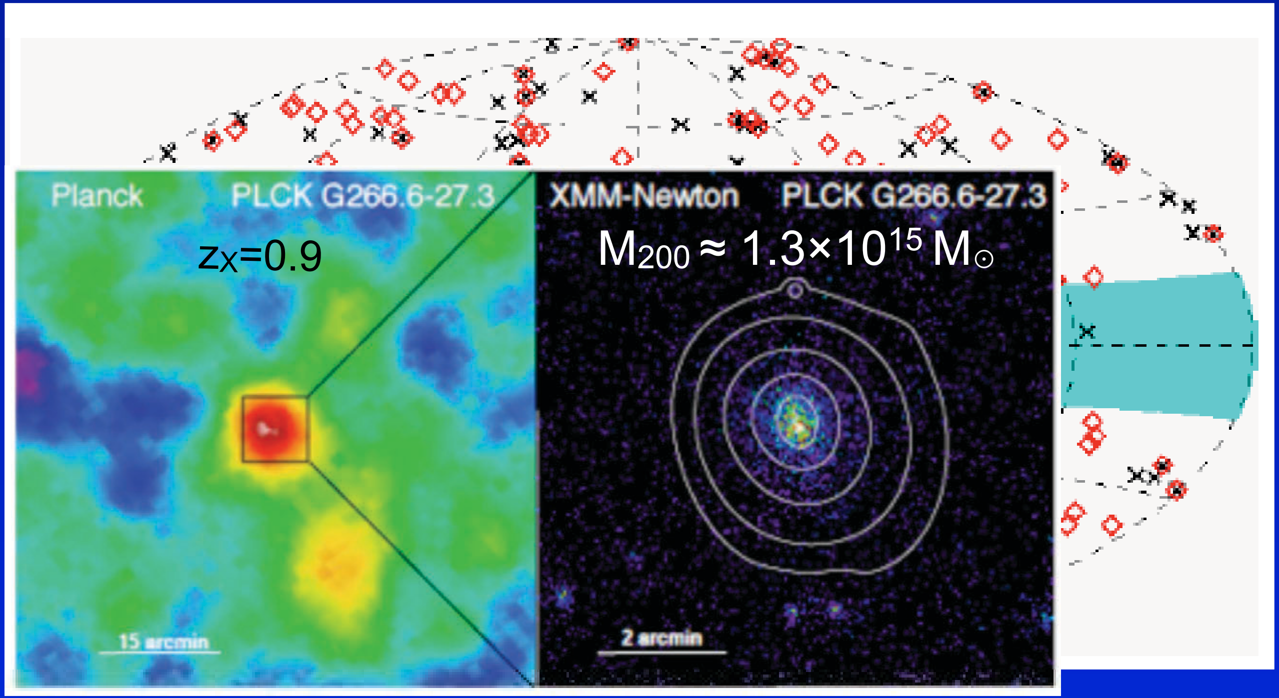

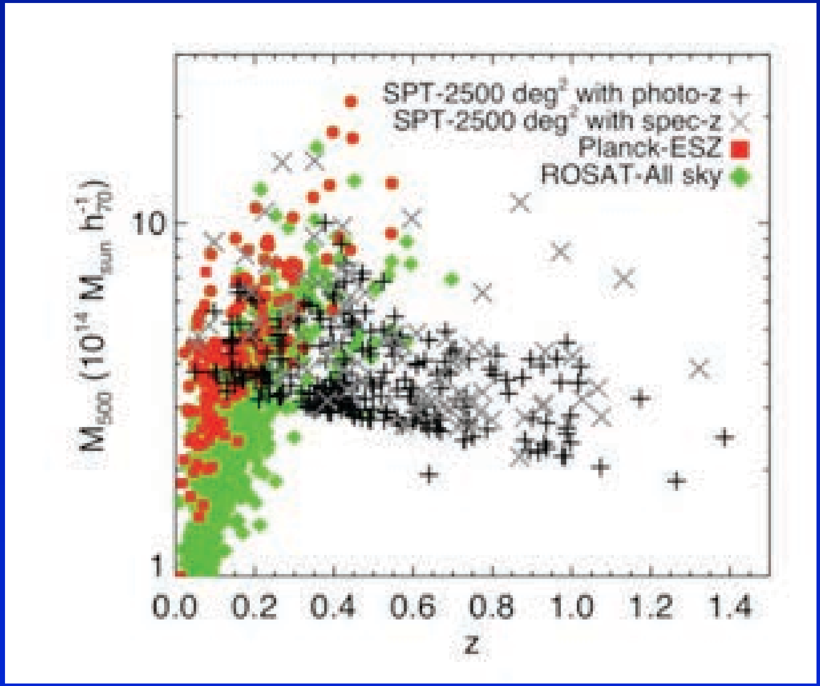

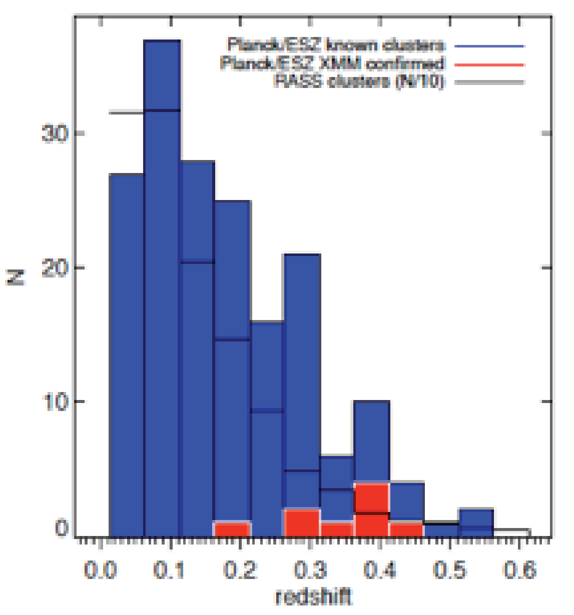

- All-sky (|b|>14 deg) SZ cluster survey (~5' beam)
- 189 clusters (S/N>6, 6 frequencies), 20 new
- Most at z<0.3, massive (>10^{14} $M_\odot$), out to z~1
- Excellence reference low-z sample once characterized
- **Larger diversity (low-Lx, merging system) compared to X-ray sample (RASS)**

Cluster Samples (1980 - 2012 .... 2020)
Summary from all methods

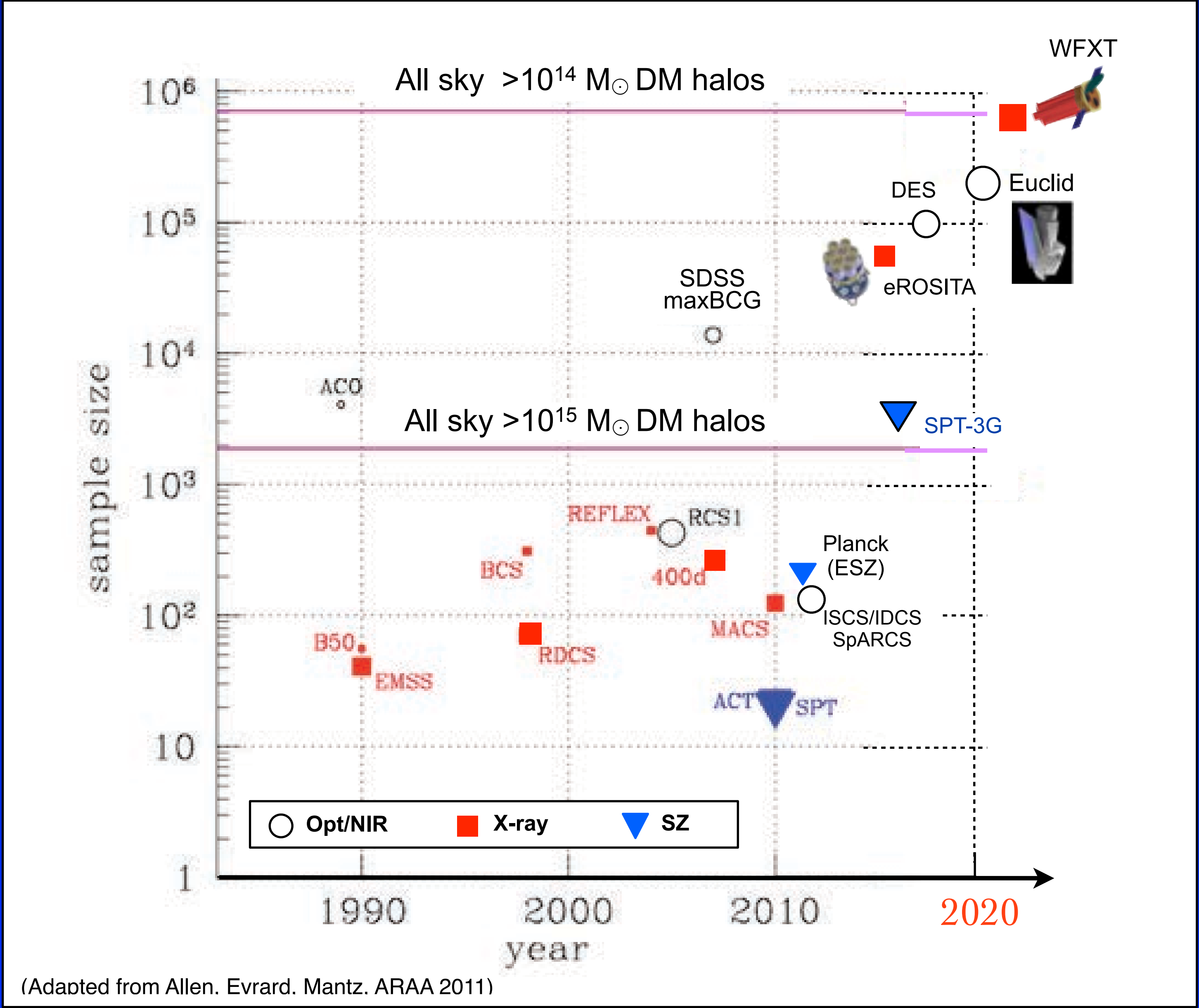

(Adapted from Allen, Evrard, Mantz, ARAA 2011)